1-1-2006

Construction of transcritical carbon dioxide air conditioning test bench.

Mowafaq Abdallah
University of Windsor

CONSTRUCTION OF TRANSCRITICAL CARBON DIOXIDE AIR CONDITIONING TEST BENCH

by

Mowafaq Abdallah

A Thesis
Submitted to the Faculty of Graduate Studies and Research
through Mechanical, Automotive and Materials Engineering
in Partial Fulfillment of the Requirements for
the Degree of Master of Applied Science at the
University of Windsor

Windsor, Ontario, Canada

2006

Your file Votre référence
ISBN: 978-0-494-42333-2
Our file Notre référence
ISBN: 978-0-494-42333-2

ABSTRACT

Carbon dioxide was widely used as a refrigerant during the last part of the 19th century and first part of the 20th century. However it fell out of use after the introduction of CFCs in the early 1930s. After the CFCs and the HCFCs were deemed unfit as working fluid in refrigeration, air conditioning and heat pump applications because of their impact on the global environmental, there has been a renaissance for carbon dioxide technology. In order to carry out a research in this field, CO_2 air conditioning test bench was constructed in the University of Windsor. This test facility is a unique and novel facility, which is the first one of its kind in Canada.

Dedicated to my-

beloved parents,

wife Amal,

sons Ahmad and Mostafa,

and daughter Zahra

ACKNOWLEDGEMENTS

The author would like to thank and acknowledge his sincere gratitude to Dr. A. Fartaj and Dr. D. S-K. Ting for their supervision, support and guidance throughout the research work. Without their advice and encouragement this work would not have been completed.

The author would like to extend his thank to Engineer Mesbah Khan for his support in the setting of the data acquisition system.

The author would like to thank Mr. P. Seguin for his technical support in the electronic and instruments works.

The author also would like to thank Mr. Steve and Mr. Danny in the Technical Support Center for their efforts in fabricating the water tank of the gas cooler, and the evaporator chamber.

Last but not least the author is indebted to his family for their continued support, encouragement and patience during the study period.

TABLE OF CONTENTS

ABSTRACT iii

DEDICATION iv

ACKNOWLEDGMENTS v

LIST OF TABLES x

LIST OF FIGURES xi

NOMENCLATURE xiv

CHAPTER

1. INTRODUCTION 1

1.1 History of Refrigerants 1

1.2 Ozone Depletion and Global Warming 2

1.3 Carbon Dioxide, the Unique Natural Refrigerant 4

1.4 Literature Review 5

1.5 Objective of Study 7

2. TRANSCRITICAL CARBON DIOXIDE REFRIGERATION CYCLE 9

2.1 Refrigeration Cycle 9

2.2 Thermophysical Properties of CO2 10

2.2.1 Thermodynamic Properties 10

2.2.2 Transport Properties 12

2.2.3 Comparison Between CO2 and Conventional Refrigerants Properties 14

2.3 Principles of Transcritical CO2 Cycle 18

3. COMPONENTS OF REFRIGERATION SYSTEM 21

3.1 Compressor 21

3.1.1 Design of an Efficient CO2 Compressor 23

3.1.2 Influence of Different Parameters on System Performance 24

3.1.2.1 Effect of Mass Charge 25

3.1.2.2 Effect of Compressor Discharge Pressure 27

3.1.2.3 Effect of Evaporator Outlet Pressure 28

3.2 Gas Cooler 29

3.2.1 Approach Temperature and its Importance 31

3.3 Evaporator 32

3.4 Internal Heat Exchanger 33

3.5 Accumulator 33

3.6 Expansion Valve 33

3.6.1 Types of Expansion Valve 34

3.6.1.1 Orifice Tube 34

3.6.1.2 Thermal Expansion valve 34

3.6.1.3 Solenoid valve 35

3.6.1.4 Electronic Expansion valve 35

3.6.2 High Side Pressure regulator 36

4. SYSTEM DESIGN AND EXPERIMENTAL SETUP 37

4.1 Closed Loop Thermal Wind Tunnel 38

4.2 System Components 47

4.2.1 Compressor 47

4.2.2 Gas Cooler 49

4.2.3 Evaporator 51

4.2.4 Expansion valve 53

4.2.5 Accumulator 53

4.2.6 Internal Heat Exchanger 54

4.2.7 Tubing, Fittings and Flexible Hoses 55

4.2.8 Valves 56

4.2.9 Filter Dryer 56

4.2.10 Instruments 57

4.3 Experimental Procedure and Sample Calculations 59

5. CONCLUSION AND RECOMMENDATIONS 64

5.1 Conclusion 64

5.2 Recommendation 64

REFERENCES 65

APPENDIX A 69

A.1 Uncertainty in Measurement of Refrigerant Temperature 70

A.2 Uncertainty in Measurement of Air Temperature 70

A.3 Uncertainty in Measurement of Water Temperature 71

A.4 Uncertainty in Measurement of Water Mass Flow Rate 72

A.4.1 Uncertainty in Using Bucket and Weigh 72

A.4.2 Uncertainty in Using Stopwatch 72

A.5 Uncertainty in Measurement of Refrigerant Pressure 72

A.6 Uncertainty in Measurement of Refrigerant Mass Flow Rate 73

VITA AUCTORIS 74

LIST OF TABLES

Tables	Descriptions	Page
1.1	Environmental effect of refrigerants	4
2.1	Characteristics of some refrigerants	14
4.1	Description of components and measuring sensors-CO_2 circuit	40
4.2	Description of components and measuring sensors-gas cooler and evaporator	44
4.3	Specification of electric motor	49
4.4	Gas cooler data	51
4.5	Evaporator data	52
4.6	Accumulator data	53
4.7	Sample of data representing one operating condition	60
4.8	Refrigerant properties throughout the refrigeration cycle	61

LIST OF FIGURES

Figures	Descriptions	Page
2.1	Temperature entropy diagram for CO_2 transcritical cycle	9
2.2	Enthalpy and entropy changes of CO_2 in gas cooling process (a) Enthalpy change, (b) Entropy change	11
2.3	Specific heat of CO_2 as a function of temperature	11
2.4	Density of CO_2 as a function of temperature	12
2.5	Transport properties of CO_2, (a) thermal conductivity, (b) viscosity	13
2.6	Vapor pressure for refrigerants	15
2.7	Slope of saturation pressure curve for refrigerants	15
2.8	Ratio of liquid to vapor density at saturation for refrigerants	16
2.9	Volumetric refrigeration capacity for refrigerants	17
2.10	Surface tension for refrigerants	17
2.11	Transcritical cycle in the CO_2 pressure-enthalpy diagram	18
2.12	Influence of varying high-side pressure on specific refrigerating capacity (q_o), specific compressor work (w), and COP in a transcritical CO_2 cycle	19
3.1	Conventional type of connecting rod of a reciprocating compressor	22
3.2	The intake and exhaust strokes of the reciprocating piston	23
3.3	Effect of CO_2 mass charge on the system performance	25
3.4	Refrigeration cycle with the progress of CO_2 charge	26
3.5	Transformation of P-h diagram with the progress of CO_2 charge	26
3.6	Influence of compressor discharge pressure on COP, capacity and compressor power	27

3.7	Influence of evaporator outlet pressure on the COP, capacity and compressor power	28
3.8	COP versus gas cooler exit temperature	31
3.9	Temperature profile and approach temperature for cross flow HCFC-22 and CO_2 condensers	32
3.10	Pressure enthalpy diagram and flow circuit of the transcritical cycle	35
4.1	Experimental setup for transcritical CO_2 air conditioning test bench system	39
4.2	Schematic of gas cooler	43
4.3	Schematic of evaporator	43
4.4	Wind tunnel assembly	46
4.5	Heat exchanger of wind tunnel	46
4.6	The compressor	47
4.7	The drive motor cart	48
4.8	Schematic of water cooled gas cooler	49
4.9	Schematic of heat exchanger (gas cooler)	50
4.10	Gas cooler before fixing inside water tank	50
4.11	Gas cooler after fixing inside water tank	51
4.12	Evaporator after fixing in the test chamber	52
4.13	Solenoid expansion valve	53
4.14	Accumulator	54
4.15	Cross sections of internal heat exchanger	55
4.16	Filter dryer	56
4.17	Plug in & surface mounted RTDs	57

4.18	Pressure transducer	58
4.19	Refrigeration cycle	63
4.20	CO_2 System after completion	63

NOMENCLATURE

Letter	Definition
A/C	Air conditioning
CFCs	Chlorofluorocarbons
C_p	Specific heat at constant pressure [kJ/kg°C]
CO_2	Carbon dioxide
COP	Coefficient of performance
f	Supply frequency [Hz]
GWP	Global warming potential
h	Enthalpy [kJ/kg]
HCFC	Hydro-chlorofluorocarbon
HFC	Hydro fluorocarbon
HVAC	Heating, ventilation and air conditioning
hv	Ultraviolet (sunlight)
k	Thermal conductivity [W/m°C]
O_3	Ozone
O_2	Oxygen
O	Atom of Oxygen
ODP	Ozone depletion potential
N	Number of poles
PH	High pressure [bar]
PL	Low pressure [bar]
PDOL	Potential destruction of the ozone layer

q	Heat transfer rate [kW]
R-744	Carbon dioxide
rpm	Revolution per minutes
RTD	Resistance temperature detector
Srpm	Synchronous revolution per minutes
T	Temperature [°C]
UV	Ultraviolet ray
V	Velocity [m/s]
W	Power [kW]

Greek symbol

ρ	Density [kg/m^3]
μ	Viscosity [kg/ms]
σ	Surface tension [N/m]

Subscript

a	Air
c	Cold
comp	Compressor
ev	Evaporator
g	Gas cooler
h	Hot
i	Inlet
ihx	Internal heat exchanger

$\dot{m}$	Mass flow rate
out	Outlet
r	Refrigerant
w	Water

CHAPTER 1

1. INTRODUCTION

Chlorofluorocarbons (CFCs) have been used in the manufacturing of refrigerators, air conditioners, and other products such as foam insulations. It has been concluded by the scientists worldwide that Chlorofluorocarbons (CFCs, also known as Freon) deplete the ozone layer. When these chemicals are allowed to escape from the air conditioning systems, they drift some 30 miles above the earth to the stratospheric ozone layer, a layer that protects the earth from the biologically harmful ultraviolet radiation emitted from the sun. When the CFCs break apart, the released chlorine attacks ozone. One chlorine atom can destroy more than 100,000 ozone molecules (Center of Atmospheric Science, 1980). When ultraviolet light ($h\nu$) hits ozone it splits into a molecule of O_2 and an atomic oxygen O, that is,

$$O_3 + h\nu \rightarrow O_2 + O. \qquad (1)$$

Therefore after the Montreal Protocol in 1987, CFCs production was phased out and the CFCs have been replaced with a chlorine free refrigerant HFC (R134a).

The hydro fluorocarbon (R134a) does not destroy the ozone layer, it has zero potential destruction of the ozone layer (PDOL), but its global warming potential (GWP) is 1300 times that of carbon dioxide, because of this it should not be used in the long-term. Therefore natural refrigerants with low GWP have attracted interests of the researchers world wide, and have gained considerable attention as a long-term solution and alternative refrigerant to the synthetic refrigerants.

1.1 History of Refrigerants

Alexander Twining proposed carbon dioxide as a refrigerant for vapor compression system in 1850. Thaddeus S. G Lowe built the first carbon dioxide system in about 1869 in Jackson Mississippi. When a German engineer called Franz Windhausen, designed his carbon dioxide compressor in 1886, he brought carbon dioxide system into wide use (Liao et al. 2000). In the 20th century carbon dioxide was commonly used in the refrigeration and air conditioning industries. In the 1930s and 1940s with the introduction

of CFC (chlorofluorocarbon) and HCFC (hydro-chlorofluorocarbon) refrigerants, the use of carbon dioxide as a refrigerant in the vapor compression system was interrupted, and twenty years later fluorocarbons became major refrigerants in vapor compression refrigeration applications. The reasons behind the replacement of the carbon dioxide with the fluorocarbons were:

1. Carbon dioxide rapidly lost capacity and efficiency at high temperatures; this was more evident in case of air-cooled gas cooler instead of water-cooled.
2. The high operating pressure and the failure of the manufacturers to develop efficient and compact CO_2 compressor with low weight and low cost (Lorentzan 1995).
3. Due to the low operating pressure of the fluorocarbons low cost components and tube assembly can be used.
4. The fluorocarbons were considered to be non-toxic to the human and harmless to the environment.
5. Heat rejecting pressures of the fluorocarbons are lower than that of carbon dioxide, thus they require less compressor work, which in turn led to better efficiency (Douglas and Eckhard 1998).

Only ammonia has remained the preferred refrigerant in large industrial machines, while all other conventional fields of application were then completely dominated by the various types of CFC and HCFC.

1.2 Ozone Depletion and Global Warming

The earth's atmosphere is composed of several layers. We live in the troposphere, where most of the weather occurs, such as rain, snow and cloud. Above troposphere is the stratosphere, an important region in which the ozone hole and global warming originated. Ozone is created when ultraviolet radiation ($h\nu$) strikes the stratosphere, dissociating (or splitting) oxygen molecules (O_2) into atomic oxygen (O). The atomic oxygen quickly combines with further oxygen molecules to form ozone,

$$O_2 + h\nu \rightarrow O + O, \quad (2)$$

$$O + O_2 \rightarrow O_3. \quad (3)$$

The ozone molecule is also unstable (although in the stratosphere, long lived) and when ultraviolet light strikes ozone it splits in to a molecule of O_2 and an atomic oxygen, a continuing process called the ozone-oxygen cycle. Although the concentration of ozone in the ozone layer is very small, it is vitally important to life because it absorbs biologically harmful ultraviolet (UV) radiation emitted from the sun. UV that would be very harmful to human is entirely screened out by ozone at around 35 km altitude (Centre for Atmospheric Science 1980).

Over Antarctica stratosphere ozone has been depleted over the last 15 years at certain times of the years. This is mainly due to the release of manmade chemicals containing Chlorine such as CFC's chlorofluorocarbons, and also compounds containing Bromine. CFC's are a common industrial product used in refrigeration systems, air conditioning and solvents.

The global warming potential (GWP) is an index that relates the potency of a greenhouse gas to the CO_2 emission over 100 years period. The carbon dioxide along with methane, nitrous oxide, and chlorofluorocarbons trap the heat before it can escape, causing the Greenhouse Effect, causing the global warming.

In 1974, two American scientists (Ronald and Molina) published their famous ozone depletion hypothesis, and presented their discovery that CFCs would destroy the stratospheric ozone layer of the Earth's atmosphere (Molina and Rowland 1974). On 1987, the Montreal protocol was signed to regulate the production and trade of ozone depleting substances.

Owing to the CFCs and HCFCs negative impact on the global environment, they are now phased out and replaced by the HFCs (hydro-fluorocarbons). The HCFs (hydro-fluorocarbons) are not reactive with ozone, but they are synthetic compounds foreign to the nature and have relatively high global warming potential (GWP) (Liao et al 2000). The high global warming potential of the HFCs and their unknown global environmental effect have introduced a rising attention to the use of natural substances which have a low or zero GWP and zero ODP such as carbon dioxide, ammonia, hydrocarbons, water and air as refrigerants (Liao et al 2000). Table 1.1 shows the environmental effects of the synthetic and natural refrigerants.

Table 1.1 Environmental Effects of Refrigerants (Hwang Y. 1997)

Refrigerants		Ozone Depletion Potential (ODP)	Global Warming Potential (GWP) (Time horizons of 100 years)
CFCs	CFC-11	1	4000
	CFC12	1	8500
HCFCs	HCFC-22	0.055	1700
	HCFC-141b	0.11	630
	HCFC-142b	0.065	2000
HFCs	HFC-134a	0	1300
	R-407C(HFC-32/125/134A)	0	1600
	R-410A (HFC-32/125)	0	2200
Natural Refrigerants	Carbon Dioxide (R-744)	0	1
	Ammonia (R-717)	0	0
	Isobutene (HC-600a)	0	3
	Propane (HC-290)	0	3
	Cyclopentane	0	3

1.3 Carbon Dioxide, the Unique Natural Refrigerant

Carbon dioxide was widely used as a refrigerant in the 1930s and 1940s in ships refrigerators and other stationary refrigeration systems. It was replaced by CFCs when they were introduced in the 1930s and 1940s. The discovery of (Ronald and Molina) on 1974 resulted in a search for alternative to the CFCs refrigerants. HFCs and HFC blends seems to be possible alternative to the CFC and HCFC since they have zero ozone depleting potential. The HFCs thermal and transport properties are similar to the HCFCs and CFCs properties, so they may be used with the HCFCs and CFCs machines with minor modifications (Kim and Kim 2002), but the HFCs have relatively high global warming potential, and they are synthetic compound and foreign to the nature.

As suggested by Lorentzen, carbon dioxide is a good refrigerant, since it is non flammable, non-toxic, does not effect the environments, easily available, and has excellent thermo-physical properties. He proposed the use of transcritical compression

cycle with carbon dioxide for several applications, such as automobile air conditioning and heat pumps.

There is no doubt that the available natural refrigerants: ammonia, propane and carbon dioxide can practically serve all normal refrigeration and heat pump needs in the future, and they are sufficient to satisfy normal requirements. A concentrated effort is required to recover lost development during half a century of halocarbon domination. One of the most important reasons behind the revival of CO_2 is the advancement in manufacturing techniques and materials. After years of development the compressor and heat exchanger technology has reached an advanced stage, compressors with less wall thickness and smaller size now can be produced, as well as michrochannel heat exchangers, which are smaller in size and working at higher operating pressure. As a result, a better and more energy-efficient CO_2 system can be expected.

The use of the carbon dioxide as a refrigerant in automobile air conditioning, heat pumps and residential air conditioning has been experimentally investigated in the recent years. The experimental results showed very competitive performance of CO_2 system to the halocarbons system (Lorentzan 1995).

1.4 Literature Review

Increasing focus on the environmental impact of the fluorocarbon refrigerants had led to extensive experimental and theoretical study in using carbon dioxide as a refrigerant especially in mobile air conditioning and heat pumps applications.

Lorentzen and Pettersen 1993 developed and extensively tested a laboratory prototype CO_2 automotive air conditioning system. A commercially available R12 automotive air conditioning system was used as a base line. They built a prototype CO_2 system of comparable cooling capacity. The CO_2 system included an internal heat exchanger to exchange heat between the high pressure (hot supercritical) CO_2 and low pressure (cold low density) CO_2. The displacement volume and speed of the compressor were adjusted to match the cooling capacity. A manually controlled expansion valve was used. The face area of the CO_2 evaporator and gas cooler were the same as that of the R12 evaporator and condenser. The air side surface area of the CO_2 evaporator was 25% larger than that of R12 evaporator, and the refrigerant side surface area of the CO_2

evaporator was 48% smaller than that of the R12 evaporator. The air side surface area of the CO_2 gas cooler was 34% larger than that of the R12 condenser, and the refrigerant side surface area of the CO_2 gas cooler was 41% smaller than that of the R12 condenser. It was demonstrated by the authors that the performance of the CO_2 system was comparable to the performance of the R12 system.

Hwang 1997 constructed a laboratory prototype water chiller using CO_2 as a refrigerant. A vapor compression cycle model for R22 and transcritical cycle model for CO_2 were developed and used. The performance of CO_2 was compared with that of R22 for water chilling and water heating applications. It was concluded that the capacity of CO_2 is better than that of R22 water chiller by 1 to 6%, and the COP of CO_2 ranged from -6 to +6% from that of R22 water chiller. The water heating capacity and COP was approximately 10% better than R22.

Boewe et al. 1999 experimentally investigated the performance of the transcritical R744 air conditioning system and compared the results to an R134a Ford Escort mobile air conditioning system. The R134a system was of an available size in the US, European and Japanese markets. Heat exchangers of the conventional type were used in the R134a system while microchannel heat exchangers (evaporator and gas cooler) were used in the CO_2 system. The CO_2 system had an internal heat exchanger and a manual metering valve. For the CO_2 system three types of evaporators have the same dimensions were used, they have different number of passes and different number of tubes in each pass. In both systems the face area, package volume and airside pressure drop of the evaporators and (gas cooler/condenser) were the same. For the CO_2 system three types of gas coolers have the same dimensions were used, they have different number of passes and different number of tubes in each pass. The CO_2 system was compared to the R134a system at high ambient temperature (above 45°C), the test results showed that CO_2 system gave slightly lower capacity and COP. They investigated also the influence of the internal heat exchanger on the capacity and COP of the CO_2 system. The CO_2 system was tested without internal heat exchanger and with internal heat exchanger of three different lengths 1.0 m, 1.5 m and 2.0 m. Test results showed that the use of the internal heat exchanger in the CO_2 system significantly enhanced the system performance, it increased

efficiency up to 25% and both capacity and COP, and reduced the high-side pressure for optimum performance.

Preissner et al. 2000, constructed a CO_2 and R134a air conditioning system, they compared their performance and presented the experimental results for both systems. The evaporator and condenser/gas cooler of both systems were of comparable size, and both systems had an internal heat exchanger. The compressor of the R134a system was with a fixed displacement volume of 155 cm^3, and the CO_2 compressor had a fixed displacement volume of 20.7 cm^3. Heat exchangers (evaporator and condenser/gas cooler) of latest technology (microchannel) were used in both systems. The test were carried out at different compressor speeds and ambient temperatures, the experimental results showed that comparing to the R134a system the capacity of the CO_2 system ranged from 13% lower to 20% higher, while the COP ranged from 11% to 23% lower.

1.5 Objective of Study

Due to the global warming impact of HFC automotive air conditioning, much interest has been focused on the transcritical CO_2 refrigeration system for its inherent environmental advantages. Efficient use of this system is of pressing concern to the present automotive and HVAC industries. Comparing to the phase change condensing process of conventional refrigeration cycle, the different nature of the gas cooling process leads to significantly more complicate transcritical CO_2 refrigeration cycle. In order to well understand the characteristics of this transcritical cycle and finally to establish design guidelines for an efficient automotive air conditioning system, a laboratory setup on transcritical CO_2 test bench is being developed. The test bench is a first of its kind in Canada. The research projects to be conducted on the test bench are of great needs to present Automotive and HVAC industry for the responsibility in saving our environment.

The objective of this study is divided into two parts:

1. Design and construct the test rig of transcritical CO_2 refrigeration cycle and specifying and collecting all system components, measuring devices and equipment.
2. Determine

- The heat transfer rate (q) of the CO_2 side to H_2O by conducting experiments on the thermodynamic process in the gas cooler.
- The cooling capacity of the cycle.
- COP of the cycle.
- Compressor work and power.

CHAPTER 2

2. TRANSCRITICAL CARBON DIOXIDE REFRIGERATION CYCLE

2.1 Refrigeration Cycle

The CO_2 air conditioning system consists of an evaporator, a compressor, a gas cooler, an expansion valve, an internal heat exchanger and a suction line accumulator. The refrigeration cycle on the entropy temperature diagram is shown in Fig. 2.1.

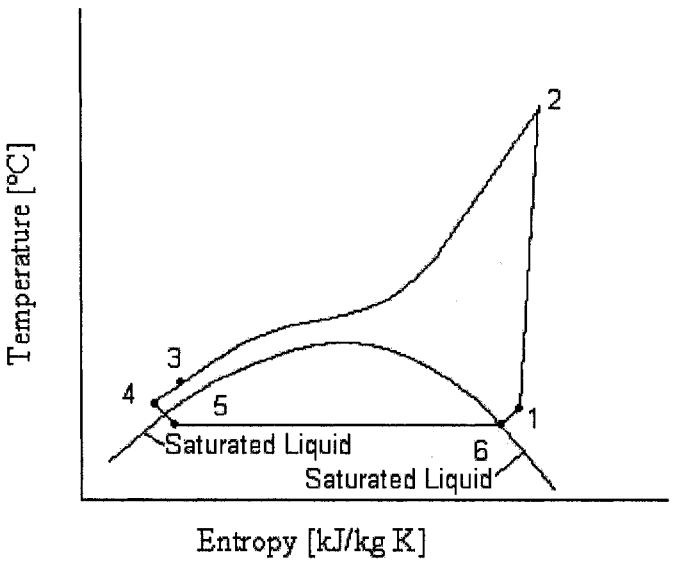

Fig. 2.1 Temperature Entropy diagram for CO_2 transcritical cycle

The compressor draws in refrigerant gas from the evaporator, compresses the refrigerant gas from a low-pressure vapor to a superheated high-pressure vapor (1-2), and discharges the compressed gas to the gas cooler. The superheated refrigerant enters the gas cooler where it rejects energy to the air that passes through the gas cooler (2-3). The refrigerant is then throttled via the expansion valve to a low-pressure two-phase mixture (4-5). In the evaporator the refrigerant absorbs heat from the air conditioned space and exits the evaporator as a two-phase mixture or as a vapor depending on the amount of energy absorbed from the air that passes through the evaporator (5-6). Then the hot supercritical fluid leaves the gas cooler and flows in the inner tube of the internal heat

exchanger (3-4), while the cold low-density fluid leaves the evaporator and flows into the accumulator and then into the outer tube of the internal heat exchanger (6-1). The compressor draws vapor from the internal heat exchanger and begins the cycle all over again.

2.2 Thermophysical Properties of CO_2

The refrigerant properties are important for the design of the air conditioning and heat pump systems as well as their components.

2.2.1 Thermodynamic Properties

One of the most important characteristics of CO_2 near the critical point is that, its properties change rapidly with temperature in an isobaric process. There are large changes in enthalpy, entropy, density, and viscosity as they approach the critical point (Kim et al, 2004). Fig. 2.2(a,b) illustrates enthalpy and entropy changes versus temperature at constant pressures. In the supercritical region the enthalpy and entropy change rapidly with temperature near the critical point. The effect of the pressure change on the enthalpy and entropy is greater above the critical temperature than below the critical temperature.

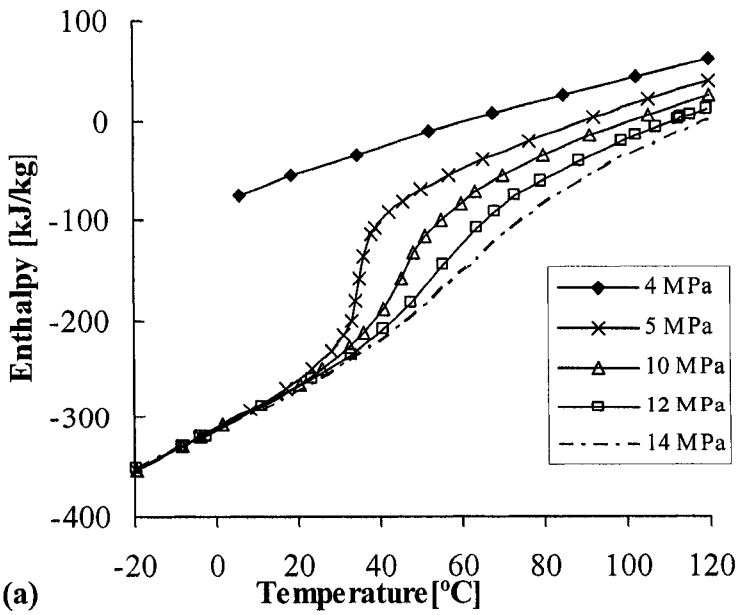

(a)

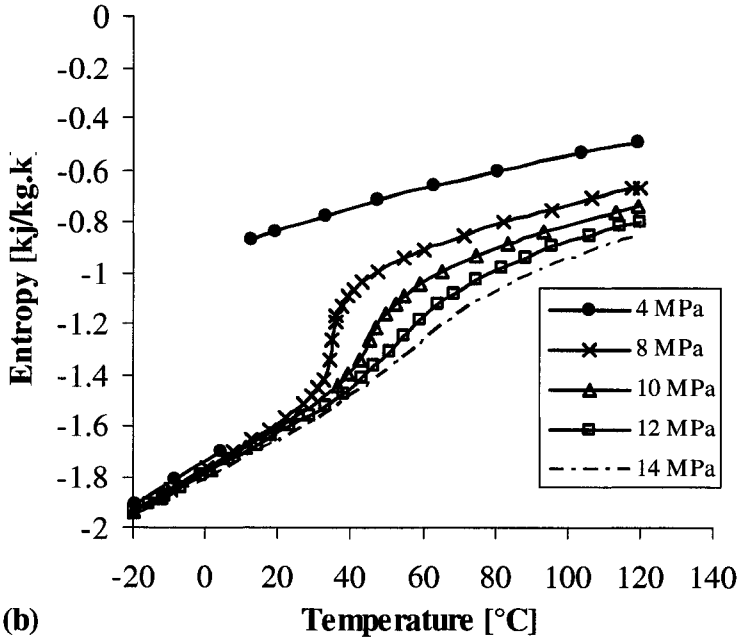

Fig. 2.2 Enthalpy and entropy changes of CO_2 in gas cooling process
(a) Enthalpy change, (b) Entropy change.

Fig. 2.3 shows the specific heat as a function of temperature, the specific heat reaches a maximum value near the pseudocritical point in an isobaric process. The pseuducritical temperature is defined as the temperature at which the specific heat becomes a maximum value for a given pressure.

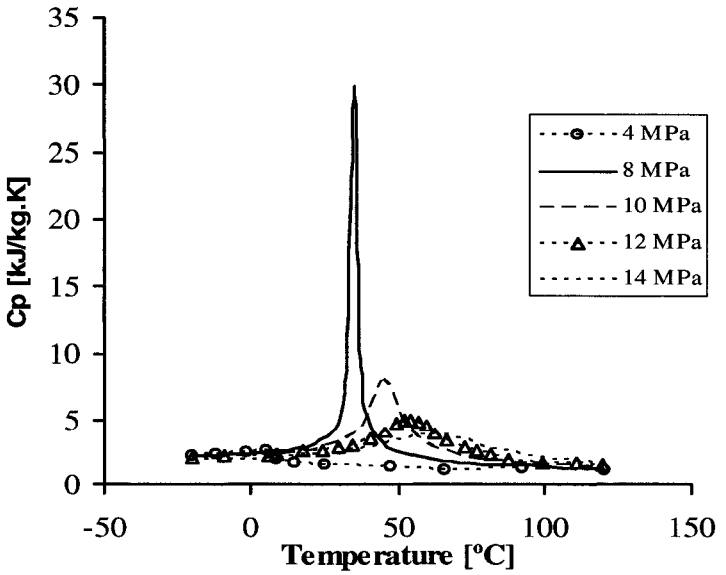

Fig. 2.3 Specific heat of CO_2 as a function of temperature.

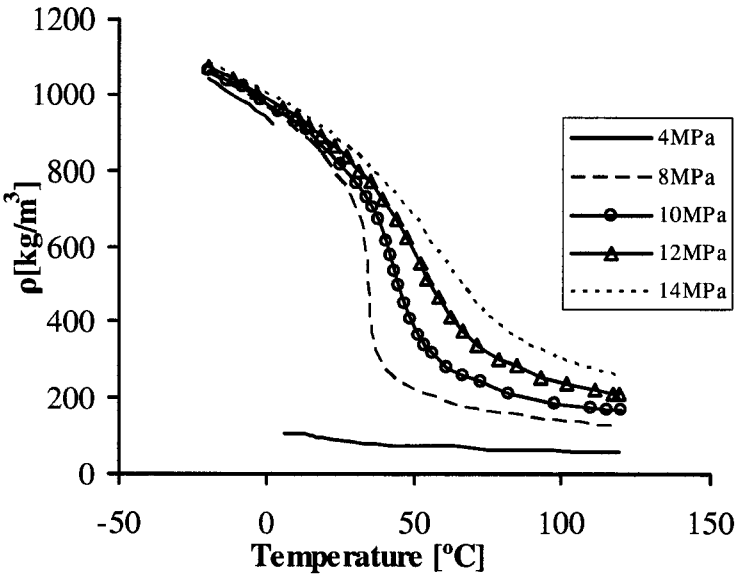

Fig. 2.4 Density of CO_2 as a function of temperature

Fig. 2.4 illustrates density of CO_2 as a function of temperature. Near the critical point the density of CO_2 changes rapidly with temperature.

2.2.2 Transport Properties

The transport properties are the viscosity and thermal conductivity. Fig.2.4 (a,b) illustrates the transport properties at supercritical and subcritical processes at varying temperatures. The thermal conductivity near the critical point increases rapidly than the viscosity. The enhancement of the thermal conductivity near the critical point is appeared in a wide range of temperature. The enhancement of the viscosity is limited to a very narrow region around the critical point (Douglas 2000).

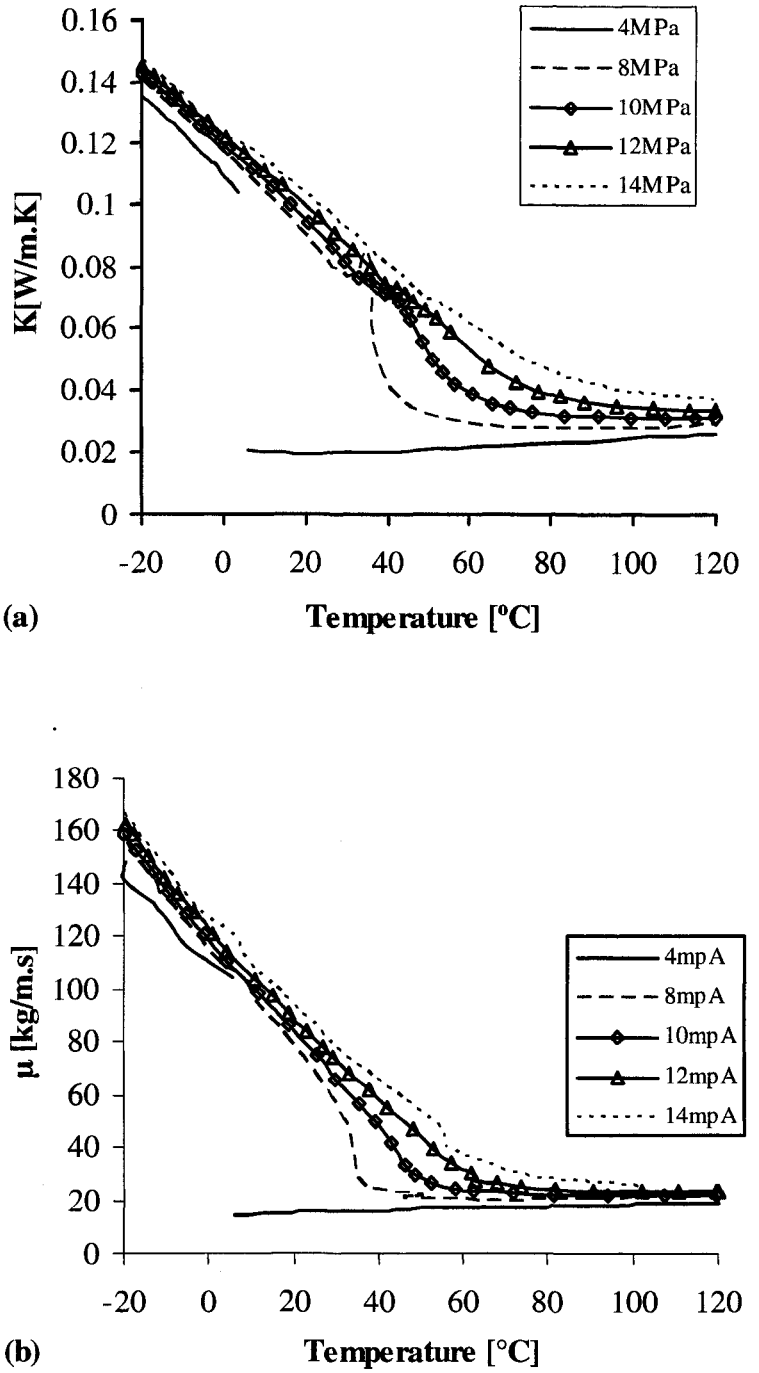

Fig. 2.5 Transport properties of CO_2. (a) Thermal conductivity, (b) Viscosity.

2.2.3 Comparison between CO_2 and Conventional Refrigerants Properties

CO_2 properties are quite different from the properties of the conventional refrigerants. The characteristics and properties of CO_2 are compared with other refrigerants in table 2.1.

Table.2.1 Characteristics of some refrigerants (Kim et al. 2004)

	R-12	R-22	R-134a	R-407C[a]	R-410A[b]	R-717	R-290	R-744
ODP/GWP[c]	1/8500	0.05/1700	0/1300	0/1600	0/1900	0/0	0/3	0/1
Flammability/ toxicity	N/N	N/N	N/N	N/N	N/N	Y/Y	Y/N	N/N
Molecular mass (kg/kmol)	120.9	86.5	102.0	86.2	72.6	17.0	44.1	44.0
Normal boiling point[d] (°C)	-29.8	-40.8	-26.2	-43.8	-52.6	-33.3	-42.1	-78.4
Critical pressure (MPa)	4.11	4.97	4.07	4.64	4.79	11.42	4.25	7.38
Critical temperature (°C)	112.0	96.0	101.1	86.1	70.2	133.0	96.7	31.1
Reduced pressure[e]	0.07	0.10	0.07	0.11	0.16	0.04	0.11	0.47
Reduced temperature[f]	0.71	0.74	0.73	0.76	0.79	0.67	0.74	0.90
Refrigeration capacity[g] (kj/m^3)	2734	4356	2868	4029	6763	4382	3907	22545
First commercial use as a refrigerant	1931	1936	1990	1998	1998	1859	?	1869

a Temary mixture of R-32/125/134a (23/25/52, %).
b Binary mixture of R-32/125 (50/50, %).
c Global warming potential in relation to 100 years integration time, from the intergovernmental Panel on climate change (IPCC).
d ASHRAE handbook 2001 fundamentals.
e Ratio of saturation pressure at 0 °C to critical pressure.
f ratio of 273.15 K (0 °C) to critical temperature in Kelvin.
g Volumetric refrigeration capacity at 0 °C.

Comparing to CFC, HCFC and HFC, CO_2 has much higher vapor pressure and its volumetric capacity (22,545 kJ/m^3 at 0°C) is 3 to 10 times larger. In the transcritical cycle the heat rejection to the ambient occurs above the critical point (critical temperature 31.1° C and critical pressure is 73.8 bars). Therefore no condensation occurs in the gas cooler. In the supercritical region the high side pressure and the temperature are not coupled, and to get the optimum operation condition they can be regulated independently.

Fig. 2.6 and 2.7 illustrate the vapor pressure and slope of the saturation pressure versus temperature of CO_2 in comparison to other fluids. As shown carbon dioxide has much higher vapor pressure than other refrigerants. The larger steepness of the vapor pressure near the critical point gives a smaller temperature change for a given pressure change.

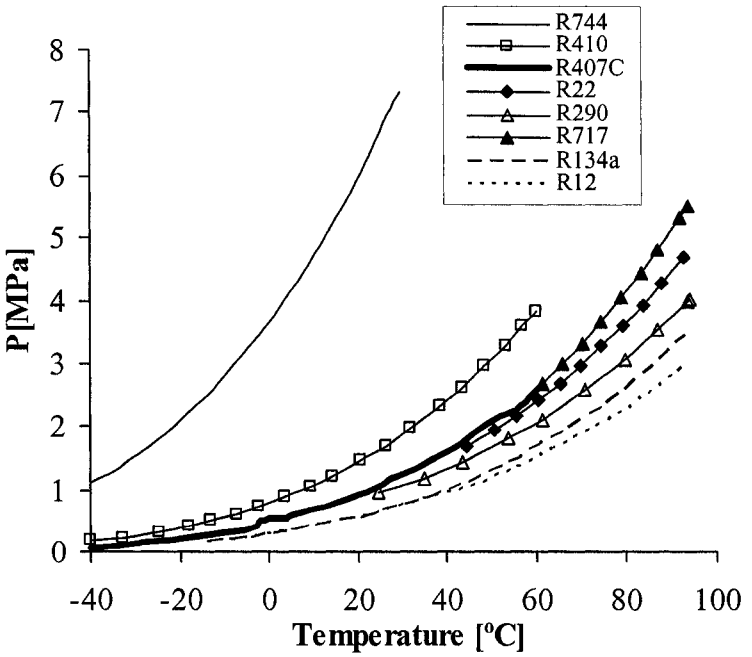

Fig. 2.6 Vapor pressure for refrigerants

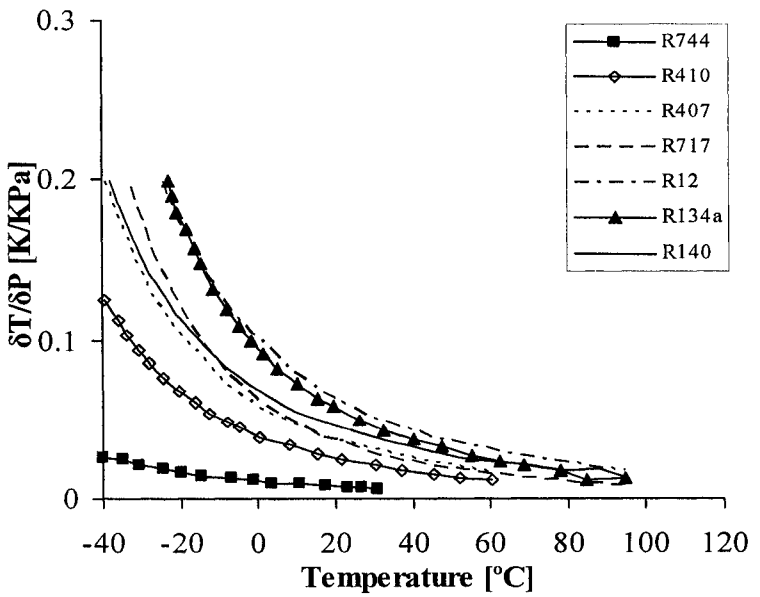

Fig. 2.7 Slope of saturation pressure curve, δT/δP for refrigerants

Thus the temperature change associated with pressure drop in the evaporator will become smaller. Due to the high vapor pressure and the closeness to the critical point, CO_2 has quite different characteristics of liquid and vapor density compared to other refrigerants.

Fig. 2.8 illustrates the ratio of liquid to vapor density for different refrigerants. The carbon dioxide density changes rapidly with temperature near critical point, it has much smaller density ratio than other refrigerants.

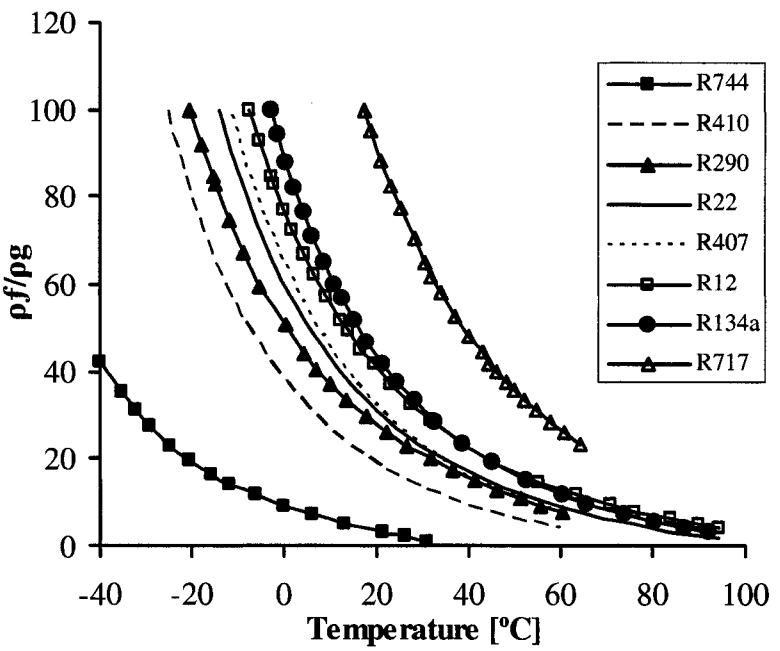

Fig. 2.8 Ratio of liquid to vapor density at saturation for refrigerants

Due to the low-density ratio of the CO_2, it has more homogenous two-phase flow compared with other refrigerants. The liquid to vapor density ratio determines the flow pattern and thus the heat transfer coefficient in the evaporator. The higher vapor density, gives the higher volumetric refrigeration capacity of CO_2. Fig. 2.9 shows the volumetric refrigeration capacity as a function of temperature. The CO_2 volumetric refrigeration capacity increases with temperature and has a maximum value at 22°C, and then drops again. The nucleate boiling and the two-phase flow characteristics are affected by the surface tension of the refrigerants. The superheat required for nucleation and growth of

vapor bubbles is reduced by small surface tension, the nucleation and growth of vapor bubbles may positively affect the heat transfer. Fig.2.10 illustrates surface tension of saturated CO_2 as a function of temperature, compared to other refrigerants. The surface tension of the refrigerants decreases with temperature and reaches zero value at critical temperature (Kim et al. 2004).

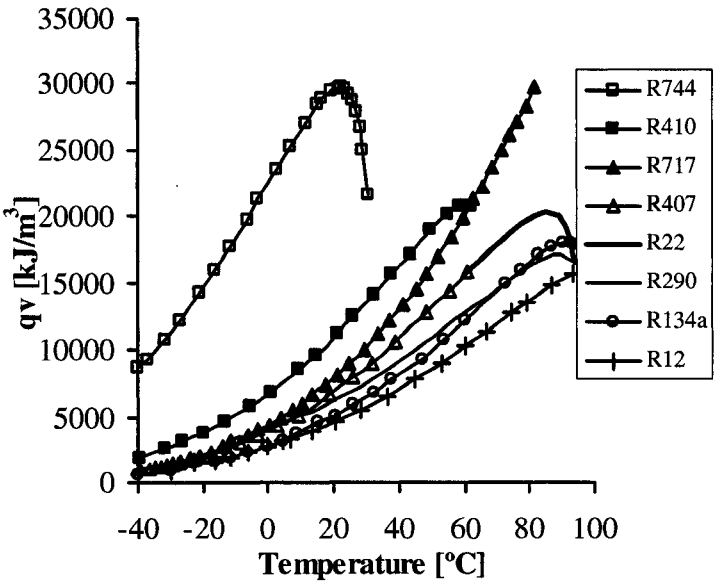

Fig. 2.9 Volumetric refrigeration capacity for refrigerants

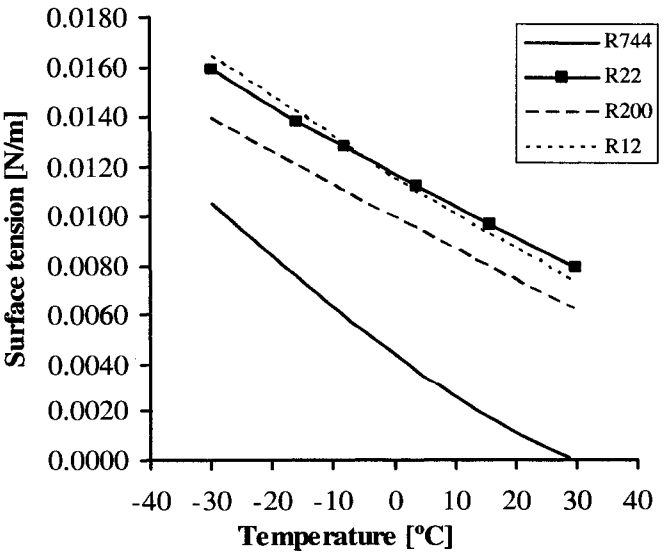

Fig. 2.10 Surface tension for refrigerants

2.3 Principles of Transcritical CO_2 Cycle

The critical point is defined as a state where no liquefaction takes place above the critical pressure and no gas is formed above the critical temperature. The fluid is in the supercritical region when both pressure and temperature exceed the critical point. The gas-cooling process of the transcritical cycle occurs when the fluid is in the supercritical region (Hwang and Radermacher 1998).

The ideal transcritical CO_2 cycle consists of four processes as shown in Fig.2.11, an isentropic compression (1-2), an isobaric heat rejection (2-3), an adiabatic expansion (3-4), and an isobaric evaporation (4-1).

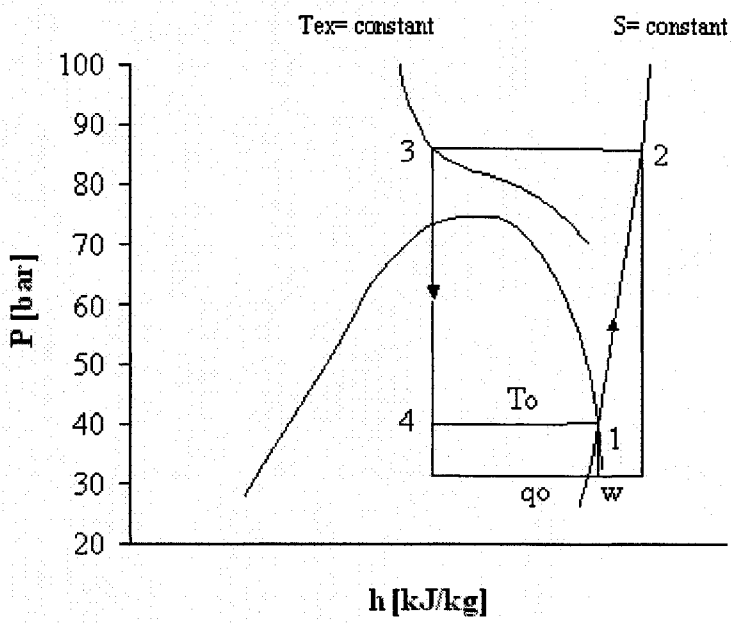

Fig. 2.11 Transcritical cycle in the CO_2 pressure-enthalpy diagram.

The critical temperature of carbon dioxide is 31.1°C; which usually is below a typical value of the heat rejection temperature of the conventional air conditioning and heat pumps systems. Due to this low critical temperature the heat rejection process takes place by cooling the compressed fluid at high-side pressure, therefore no saturation

condition takes place, while the heat absorption process occurs under the critical condition.

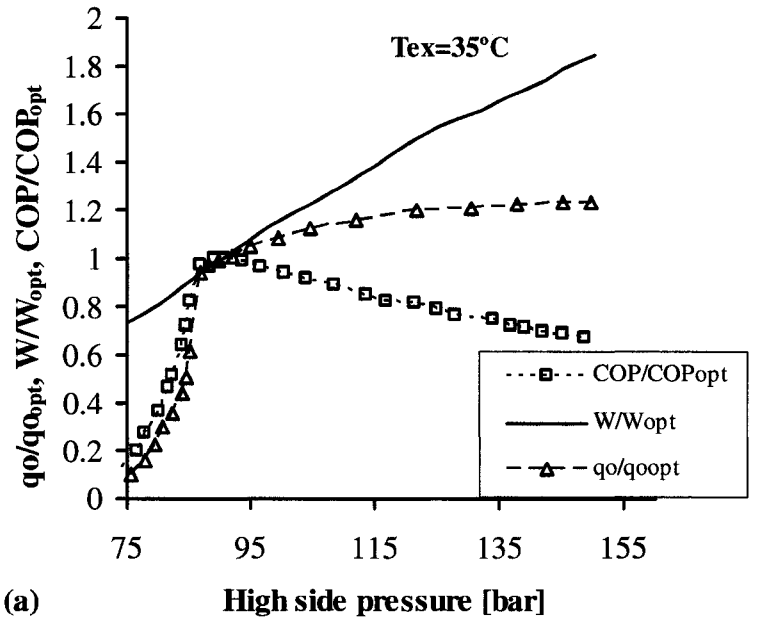

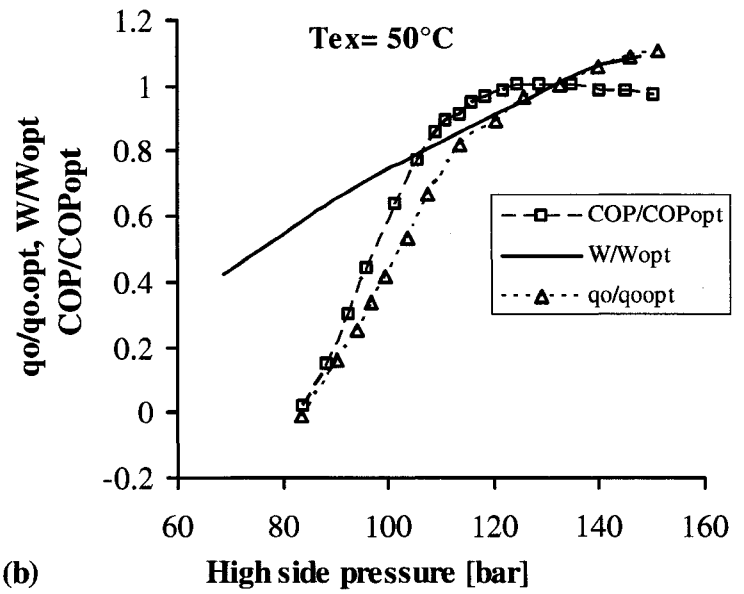

Fig. 2.12 Influence of varying high-side pressure on specific refrigerating capacity (q_o), specific compressor work (w) and COP in a transcritical CO_2 cycle.

In the conventional system, the compressor work and the coefficient of performance (COP) depend on the discharge pressure of the compressor. So COP tends to drop with increasing pressure, while in the transcritical cycle the behavior is different, as will be discussed below. The pressure is independent of the temperature at supercritical pressure, therefore the pressure has a significant influence on the enthalpy and consequently on the coefficient of performance. By regulating the high-side pressure the COP can be maintained at the maximum for a given cooling / heating capacity.

As can be seen from the Fig. 2.12(a,b), when the high-side pressure increases, the COP increases and reaches a maximum value at a certain pressure, above this point the added capacity no longer fully compensates for the additional work of compression. It is further shown that when the refrigerant outlet temperature from the gas cooler (T_{ex}) is constant at 35°C, the theoretical maximum COP is reached at 8.7 MPa, while when the refrigerant outlet temperature from the gas cooler (T_{ex}) is constant at 50°C, the theoretical maximum COP is reached at 13.1 MPa, this indicates that if the refrigerant temperature at the gas cooler exit could be reduced, the optimum pressure for maximum COP could also be reduced. In most situations, maximum capacity can be obtained at higher pressure than the optimum pressure of maximum COP (Kim et al. 2004).

CHAPTER 3

3. COMPONENTS OF REFRIGERATION SYSTEM

3.1 Compressor

The Compressors are used in the refrigeration system to compresses the refrigerant from a low-temperature and pressure to a high temperature and pressure superheated gas, and to circulate the refrigerant in the refrigeration system. These compressors range from small compressors used in automotive applications to large compressors used in residential air conditioning systems. Usually the compressor is driven by an electric motor or engine.

The transcritical CO_2 cycle operates at typical operating pressures of 100-130 bars high-and 35-50 bars low-pressure; the pressure ratio of the CO_2 system is about 3.0 (Hwang and Radermacher 1998). As compared to the conventional refrigeration systems, the pressures encountered in the CO_2 system are about 5-10 times higher, and the pressure ratio of the CO_2 system is lower due to the operation near the critical point. Because of the high operating pressure of the CO_2 system special consideration must be taken regarding the design of the components (Douglas 2000).

Due to higher-pressure level the negative effect of the valves pressure drop is small and this leads to higher compressor efficiency. And because of the high operating pressure, the CO_2 compressor needs thicker walls, but since CO_2 has large volumetric capacity the CO_2 compressor will be smaller than that of conventional refrigerant for the same capacity (Jordan and Priester 1969). For the same reason, for a given capacity the compressor displacement is reduced by 80-85% than that of conventional refrigerant.

Basically there are five types of compressors:

1. Reciprocating Compressors
2. Rotary Vane Compressors
3. Scroll Compressors
4. Screw Compressors
5. Centrifugal Compressors

The compressor of interest in this experiment is the reciprocating compressor. The reciprocating compressors are usually electric motor driven, in the automotive the power is transmitted from the engine via a belt. Reciprocating compressor may consist of one or more cylinders (Solberg and Miller 1998). The typical reciprocating compressor consist a crank a piston, a rod, a cylinder and valves.

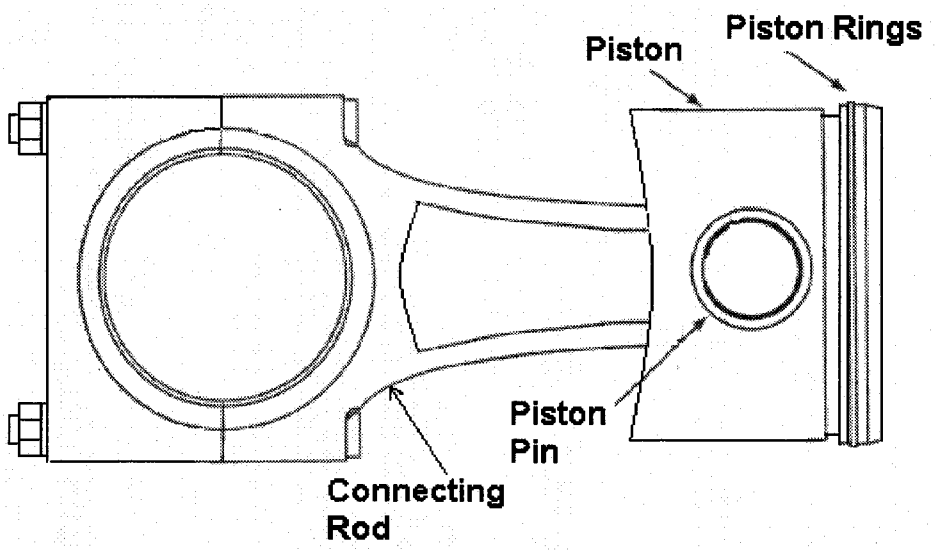

Fig. 3.1 Conventional type of connecting rod of a reciprocating compressor.

The rotary motion of the crank is changed into reciprocating motion by the connecting rod. The intake and exhaust valves are fixed in a valve plate located under the cylinder head. Fig. 3.1 illustrates a conventional type of connecting rod. The connecting rod has a big end connected to the crank and a small end connected to the piston by a piston pin. As the piston moves downward in the cylinder, the refrigerant vapor enters the cylinder from the return line through the suction valve and occupies the cylinder space. As the piston moves upward in the cylinder it compresses and pushes the refrigerant gas through the exhaust valve into the discharge line. Piston and rings used in reciprocating compressors are usually made of cast iron. The intake and exhaust stroke are illustrated in Fig. 3.2 below.

Modern automotive reciprocating piston compressor basically has two configurations, in which the pistons are driven by a wobble plate or swash plate. As the shaft rotates the (wobble/ swash) plate causes the pistons to stroke in the cylinders. The angle of the plate controls the length of the piston stroke (Süß and Kruse 1998). In a wobble plate compressor, when the drive shaft rotates an angle yoke on the drive shaft causes the plate to wobble, driving the piston in a reciprocating motion. The wobble plate is a single acting compressor. In the swash plate compressor, which is used in this work, there are no piston rods, the pistons ride on the plate. The plate is fixed to the rotating shaft, and as it rotates with the shaft it causes the pistons to reciprocate in the cylinders. The swash plate compressor is double acting (Liu et al 2005).

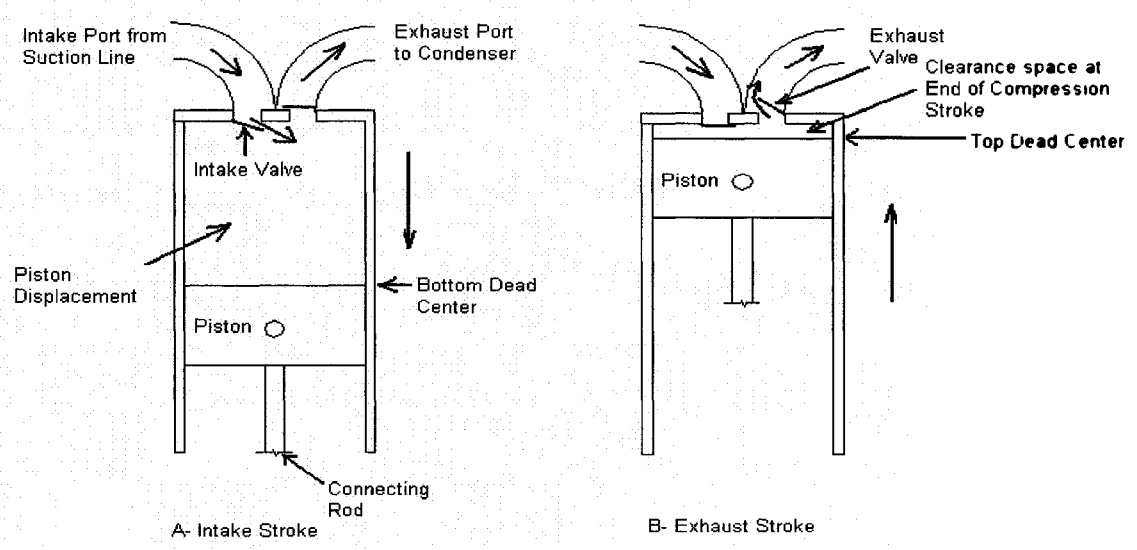

Fig. 3.2 The intake and exhaust strokes of the reciprocating piston.

3.1.1 Design of an Efficient CO_2 Compressor

CO_2 has higher vapor pressure than conventional refrigerants, which cause the compressor in the Transcritical CO_2 system, operate at high mean effective pressure. This system has a low-side pressure in range of 3-4 MPa while high-side pressure may be as high as 12-14 MPa. In the Transcritical CO_2 system the pressure ratio is low due to its operation being close to the critical point. This low-pressure ratio results in higher performance of CO_2 compressor. Moreover, due to the high pressure difference, pressure

losses inside the compressor may have strong influence on the CO_2 compressor performance, with appropriate design the effect of leakage occurring at the valves and inside the gas chambers can be reduced to a reasonable amount and compressor performance can be improved (Solberg and Miller 1998). Because of the high operating pressure of the CO_2 system special consideration regarding the components design is required. The compressor technology has reached an advanced stage after years of extensive researches and developments (Douglas 2000).

Fagerli 1997 through his investigation evaluated the possibilities to use a small hermetic compressor for transcritical compression of CO_2. He built and instrumented a single cylinder 2.6 cm^3 hermetic prototype machine with flanged shell, using dome parts from R-22 machine. The results showed that the measured isentropic efficiency (which is the ratio of the theoretical work required for the isentropic compression to the actual work required by the compressor) for the CO_2 compressor were 9-15% lower than that of R-22 machine, and the volumetric efficiency was lower by less than 5%. Since these results were in an early stage of development, they considered as promising. The predicted results from the theoretical models showed a potential for higher energy efficiency with CO_2 than with R-22. Due to the viscosity reduction caused by dissolved CO_2 in the lubricant, Fagerli used mineral oil with three times higher viscosity grade than for R-22.

Süß and Kruse 1998 investigated the parameters influencing the compressor performance. They reported that leakage of the cylinder has a major influence on the compressor performance; therefore it is important to minimize the length of leakage gaps. They focused on reciprocating compressors with piston ring; they reported that the lowest leakage rate can be achieved in this type by applying piston rings, while they consider other types of compressors (scroll, rotary, vane and rolling pistons) as a non promising option.

3.1.2 Influence of Different Parameters on System Performance

Liu et al 2005 experimentally investigated the parameters influencing the compressor performance.

3.1.2.1 Effect of CO2 Mass Charge on the System Performance

It is observed from Fig. 3.3 when the CO_2 charge increases the cooling capacity increases, due to the increase in the compressor outlet pressure compressor power increases as well. There is an optimum CO_2 charge for maximum COP. And when the CO_2 charge is less than the optimum charge it is observed that both the cooling capacity and COP decrease.

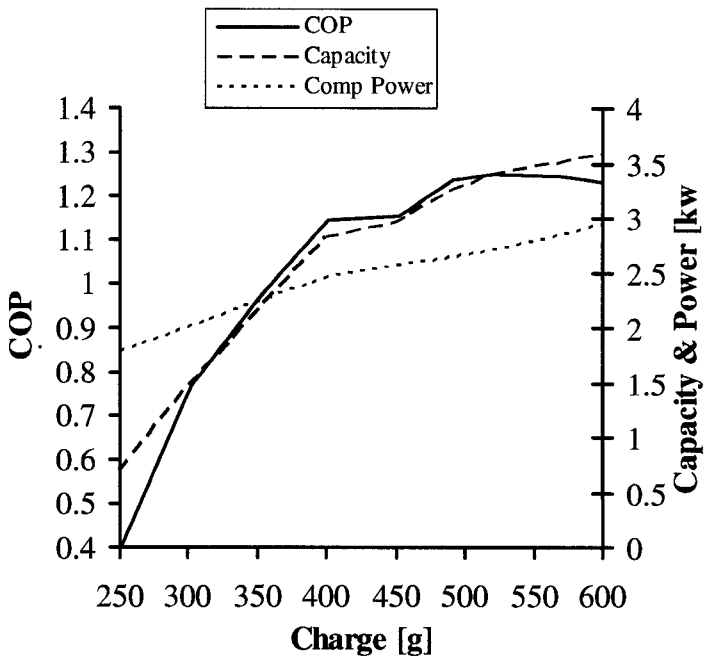

Fig. 3.3 Effect of CO_2 mass charge on the system performance

The refrigeration cycle with the progress of CO_2 charge is shown in Fig. 3.4 and 3.5, at the beginning of the charging process when a very small amount of CO_2 is charged into the system, the refrigeration cycle will be formed in the superheat zone, resulting in low compressor discharge pressure, the CO_2 in the system will be in a vapor state, and a small temperature decrease during the throttling process will be observed.

Therefore the cooling capacity for this cycle may be considered as zero. When the CO_2 charge is increased slightly the vapor temperature leaving the expansion valve will just reach the saturation line. As the CO_2 charge is gradually increased the outlet state of the expansion valve will be brought into the two-phase region, and the evaporator inlet

quality will be less than one. The compressor discharge pressure will go up higher than the critical pressure and the temperature after the throttling process before entering the evaporator will be at the design temperature. In the gas cooler the refrigerant will be at the supercritical state.

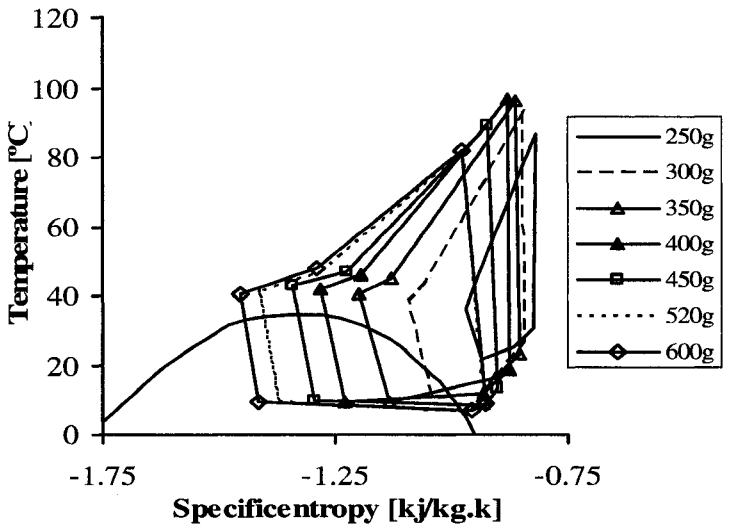

Fig. 3.4 Refrigeration cycle with the progress of CO_2 charge.

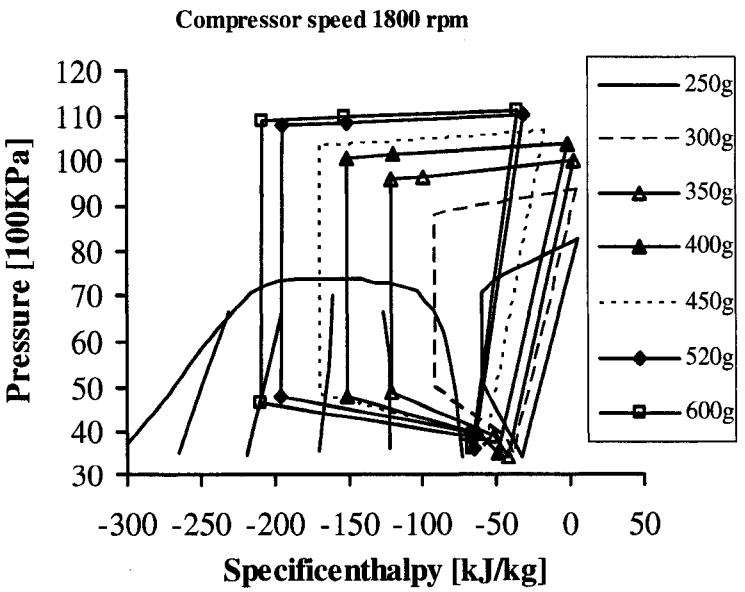

Fig. 3.5 Transformation of P-h diagram with the progress of CO_2 charge

It may be observed from Fig.3.4 and 3.5 as the CO_2 charge is increased, the discharge pressure increases, and the compressor inlet temperature decreases. In this condition the cooling capacity increases slowly, and compressor work will increase significantly. In order to avoid compressor damage, the compressor inlet temperature should be higher than the saturation temperature depending on the compressor inlet pressure.

3.1.2.2 Effect of Compressor Discharge Pressure on the System Performance

Fig. 3.6 shows the effect of the compressor discharge pressure on the system performance.

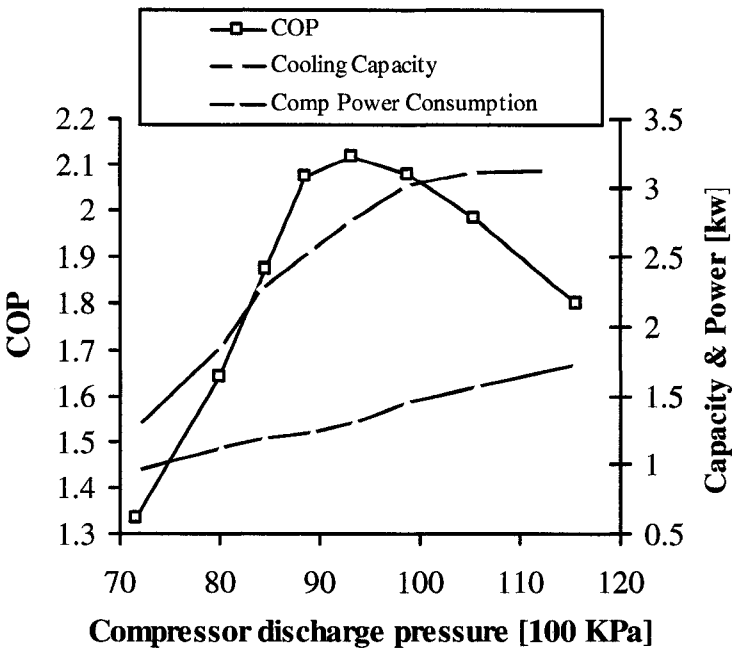

Fig. 3.6 Influence of compressor discharge pressure on COP, Capacity and Power.

During this experiment the evaporator outlet pressure manually kept constant, in this condition the compressor discharge pressure depends mainly on the CO_2 charge level. When the compressor discharge pressure increases, the compressor discharge temperature increases and the CO_2 charge required by the system increases too, the compressor inlet temperature decreases slightly, the refrigerant quality decreases and consequently the cooling capacity increases. Due to the increase in compressor discharge

pressure the compressor power increases and COP increases up to a certain point then drops down, which show that the system performance is strongly influenced by the compressor discharge pressure.

3.1.2.3 Effect of Evaporator Outlet Pressure on the System Performance

Fig. 3.7 a-c shows the effect of evaporator outlet pressure on the system performance. During this experiment adjusting the expansion valve manually changed the evaporator outlet pressure. When the expansion valve opening is manually increased the mass flow rate through the valve increases and the CO_2 will transfer from the high side pressure to the low side pressure, the high side pressure decreases resulting in the decrease of the systems capacity and COP. Because the compressor outlet pressure decreases the compressor power consumption decreases.

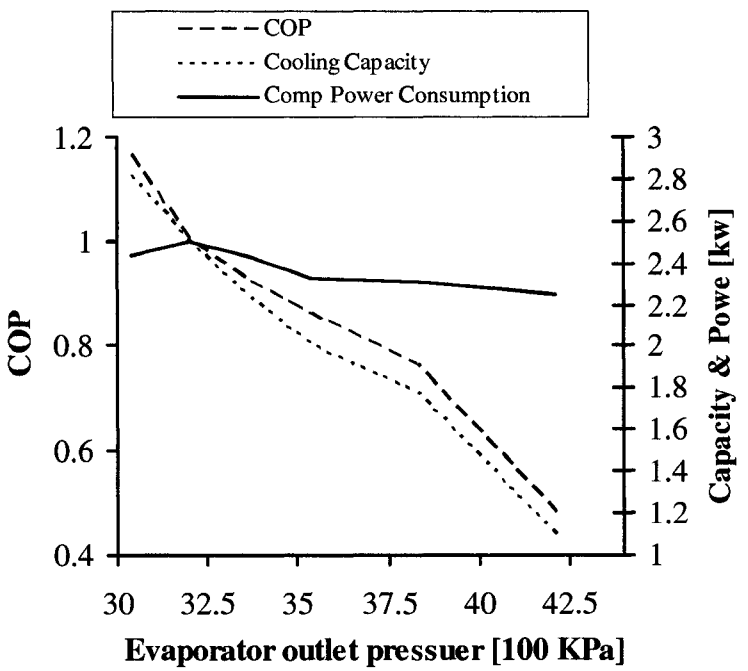

Fig. 3.7 Influence of evaporator outlet pressure on COP, Capacity and Power.

3.2 Gas Cooler

The gas cooler performs to cool the refrigerant and reject its heat to the ambient. The air conditioning system works with CO_2 as a refrigerant operates mostly in a transcritical region, where the heat rejection process takes place by cooling of single phase refrigerant in the region above the refrigerant critical temperature and pressure, the refrigerant stays in the gas state without phase changing. While in the conventional refrigeration cycle during the heat rejection process in the condenser, the refrigerant changes from gas state into the liquid state, so that the condensing phenomena takes place (Pettersen et al 1998).

One of the most important characteristics of carbon dioxide near-critical or near pseudo-critical regions is that its thermo-physical and transport properties change rapidly, especially the specific heat, it reaches its peak point near the pseudo-critical point. These changes affect the heat transfer coefficient and the pressure drop characteristics.

The variation in the specific heat (Cp) highly influences the heat transfer coefficient of a single phase fluid at supercritical pressure. Near the critical region the specific heat is relatively high and reaches its maximum value at the critical point. Other properties like thermal conductivity, density and viscosity also show irregularities near the critical point, and the heat transfer coefficient and pressure drop are affected by these irregularities. Standard single-phase heat transfer correlations, like the Gnielinski model or the standard textbook Dittus-Boelter correlation are used by most of the authors. These correlations may give inaccurate results at or near the pseudocritical state for low Reynolds numbers (Riebere and Halzon 1997).

Kuang et al. 2004 conducted experiment and investigated the heat transfer and pressure drop characteristic of supercritical gas cooling process of CO_2 in microchannels. Experiments were conducted over a range of mass flux of 300 to 1200 kg/m^2s, and for pressure ranging from 8 to 10 MPa. The experimental data were taken around pseudo-critical region. The results showed that the mass flux had significant influence both on heat transfer coefficient and pressure drop in supercritical gas cooling process. When the mass flux increases both heat transfer coefficient and pressure drop increase. Near pseudo-critical temperature, heat transfer coefficient enhances due to the high specific

heat. It is found that the conventional correlations for forced convection such as Gnielinski's correlation worked fine in low mass flux region. However they did not predict the experimental data very well in high mass flux region, especially near the pseudo-critical region with deviation as much as 60%, which is due to the effects of significant variation in thermodynamic properties in this region.

The gas cooler design has a significant influence on the system performance. The efficiency of the transcritical air conditioning and heat pump cycle is highly influenced by the gas cooler exit temperature. Results obtained from experiment carried out on a prototype mobile air conditioning system showed that, when the gas cooler exit temperature is reduced, the optimum high-side pressure decreases and the (COP) coefficient of performance increases due to the reduction in compressor power (Yin et al 2002). In the transcritical CO_2 cycle, system performance is very sensitive to gas cooler design. A small change in temperature can produce a large change in refrigerant enthalpy at the gas cooler exit because at the critical point the specific heat becomes very large (Kim et al 2004).

The relation between COP and discharge pressure at different gas cooler exit temperatures is shown in Fig 3.8. The following conclusions can be obtained from the figure.

- When the inlet temperature of the air interring gas cooler increases, the R744 gas cooler exit temperature increases, then the operating pressure required to maximizing cycle COP needs to be increased.
- When the gas cooler exit temperature decreases lower than the critical temperature (31°C) optimum COP is not exist (Yin et al 2002).

Due to the high operating pressure and the excellent heat transfer properties of CO_2, tube diameter can be reduced, and new technology of heat exchanger with flat multi port (microchannel) tubes can be employed. These reductions provide more air-side surface per unit core volume, which allow more compactness, save material weight, reduce internal volume and reduce the explosion energy (Pettersen et al 1998). This technology in comparison to the conventional flat fin/round tube heat exchanger has greater refrigerant-side area, less airside pressure drop, and higher airside heat transfer coefficient due to higher face velocities (Kim et al 2004).

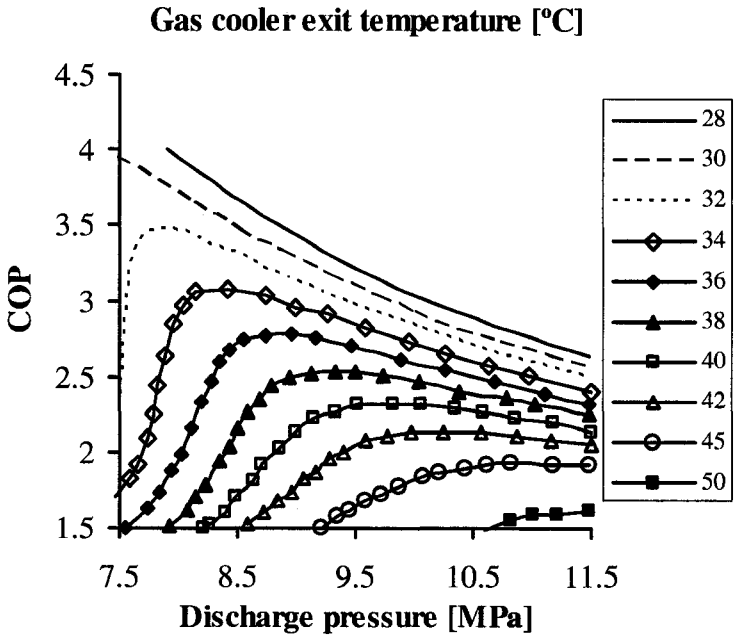

Fig. 3.8 COP versus gas cooler exit temperature

3.2.1 Approach Temperature and its Importance

The temperature approach is defined as the difference between refrigerant temperature at the gas cooler exit and air inlet temperature. Although the high specific heat at near-critical pressure is favorable for heat transfer, it gives the transcritical CO_2 cycle a large throttling loss.

The refrigerant outlet temperature from the gas cooler is very important for system COP. Heat exchanger design calculations and practical experience show that it is possible to make the refrigerant outlet temperature from gas cooler become as close to the air-or cooling water inlet temperature. Fig. 3.9 shows the difference between the temperature profile in a traditional condenser and a near-critical CO_2 cooler. The diagram is based on a cross-flow coil with 25°C air-inlet temperature with mean temperature difference of 10K. The temperature approach is reduced from 4.1 K for HCFC-22 to 1.0 K for CO_2 because of the different temperature profile, in the CO_2 the heat is rejected over a temperature glide, while in the conventional system the heat is rejected at constant temperature (Pettersen et al 1998).

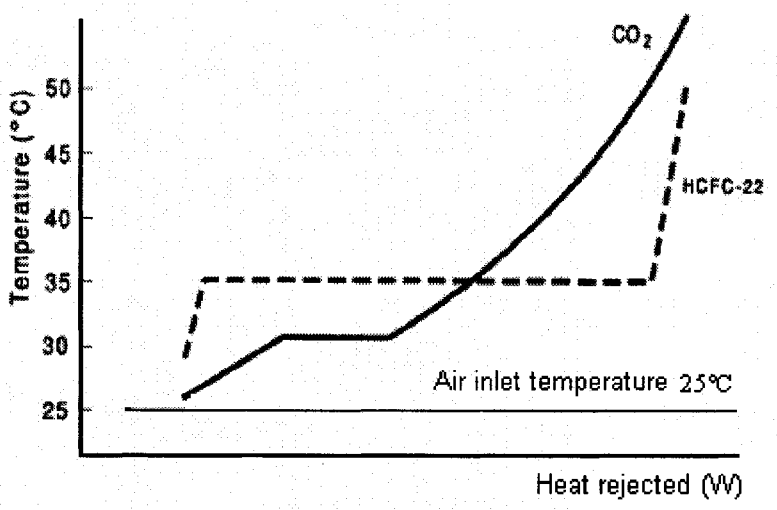

Fig. 3.9 Temperature profiles and approach temperature for cross-flow HCFC-22 and CO_2 condensers

3.3 Evaporator

The evaporator is used to remove the heat from the air-conditioned space in the recent years; researches are going on to employ the microchannel technology within the automotive air conditioning industries. The new technology (microchannel) enables higher face velocities that increase the airside heat transfer coefficient, and greater refrigerant-side area, which improve the performance of the evaporator. Compared to the plain fins, the louvered fins increase the airside heat transfer coefficient by 50-100% (Kim et al 2004). A comparison between properly designed CO_2 evaporators and baseline HFC/HCFC evaporators shows that;

- In spite of the high evaporator pressure in the CO_2 system the explosion energy (which is product of pressure and volume) is the same as the baseline evaporator, because of the reduced volume in the CO_2 system.
- CO_2 properties such as high thermal conductivity, low kinematics viscosity and high specific heat of liquid CO_2 are favorable for heat transfer behavior.
- The low liquid/vapor density ratio of CO_2 may give more homogenous two phase flow in the evaporator and this leads to better distribution of CO_2 in the evaporator.

- The smaller surface tension of CO_2 positively affects heat transfer, and improves the evaporation heat transfer coefficient (Pettersen et al 1998).

3.4 Internal Heat Exchanger

The internal heat exchanger is used to sub cool the hot refrigerant which leaves the gas cooler and to superheat the cold refrigerant which leaves the evaporator, it is an important component in the transcritical CO_2 system. Extensive experimental studies have been carried out on the benefits of the internal heat exchanger for transcritical automotive air conditioning system. Experimental results showed that internal heat exchanger has a significant effect on system performance; it can increase cycle efficiency up to 25% (Boewe et al 1999).

3.5 Accumulator

A suction accumulator is a vessel that holds the extra refrigerant-oil mixture in the system; in the CO_2 transcritical system it is installed after the evaporator, it allows the refrigerant-oil mixture to return to the compressor slowly and in small quantities to avoid a possible damage. Slugging is one of the common failures in refrigerant compressors, it occurs when liquid refrigerant returns to compressor in large quantities. The compressors are designed to compress vapors only. Some times during operation of the refrigeration system, unusual amount of refrigerant will collect in the suction accumulator, such cases happen when the system is shut off, or when the system is operated under low load conditions. In such cases the metering orifice in the lower end of the exit tube of the accumulator is quite adequate to draw in a small amount of liquid refrigerant-oil mixture from the bottom of the accumulator and deliver it to the compressor at a non-harmful rate.

3.6 Expansion Valve

The expansion valve is a device that causes a pressure drop to the liquefied refrigerant flow, sprays it into the evaporator where the pressure is low enough that it boils. The liquefied refrigerant in the evaporator absorbs the latent heat of evaporation

from the occupied space and change into gas state. The expansion valve meters the refrigerant according to the heat load in order to maintain a given superheat. Superheat is the amount of further heat added to the refrigerant in the evaporator after it has boiled. The super heat is required to evaporate the entire refrigerant in the evaporator. Any liquid refrigerant that escapes the evaporator is considered as wastage of cooling.

3.6.1 Types of Expansion Valve

3.6.1.1 Orifice Tube

The orifice tube is the most commonly used in automobiles. It is affixed metering device, it causes a pressure drop and it does not control the flow of the refrigerant. It is inexpensive, it measures approximately 3 inches in length, and it is common to get clogged with debris.

3.6.1.2 Thermal Expansion Valve

The thermal expansion valve is also a common refrigerant regulator; it regulates the flow of refrigerant according to the load. It senses evaporator pressure and temperature and control the refrigerant flow so as to maintain a given superheat. The amount of superheat in the refrigerant gas determines the valve setting. Superheat is the heat added to the refrigerant above its saturation temperature. The valve has a bulb filled with a fluid is attached to the outlet tube of the evaporator; the bulb senses the temperature of the refrigerant exiting the evaporator at this point. This bulb is connected to the valve by a tube, when the load in the system increases and the temperature of the refrigerant in the evaporator rises, then the fluid in the bulb expands and increases the valve opening to allow more refrigerant to enter the evaporator. Conversely if the load in the system decreases, then the temperature of the refrigerant in the evaporator drops down and the fluid in the bulb contracts and tends to decrease the valve opening allowing less amount of refrigerant to enter the evaporator.

3.6.1.3 Solenoid Valve

It is a power operated electromechanical valve with movable core and it is used in many refrigerating applications. An electrical signal from a simple electrical circuit controls the solenoid valve. Based on its design it is either normally closed or normally opened. It is used when automatic control of fluid flow is required. In central heating applications a solenoid valve may be activated by a signal from a thermostat.

3.6.1.4 Electronic Expansion Valve

Due to the expense of electronic expansion valves, they have not been traditionally used for automotive applications. An electronic expansion valve (EEV) system requires a computer to monitor the evaporator inlet and the outlet temperature. From this feedback, the computer actively controls the valve setting.

3.6.2 High-side Pressure Regulation

In the trnscritical cycle at supercritical conditions, the high-side pressure is independent of temperature. By regulating the high-side pressure the COP can be maintained at the maximum and/or to regulate the cooling or heating capacity (Kim et al 2004), so some kind of high-side pressure regulation is necessary.

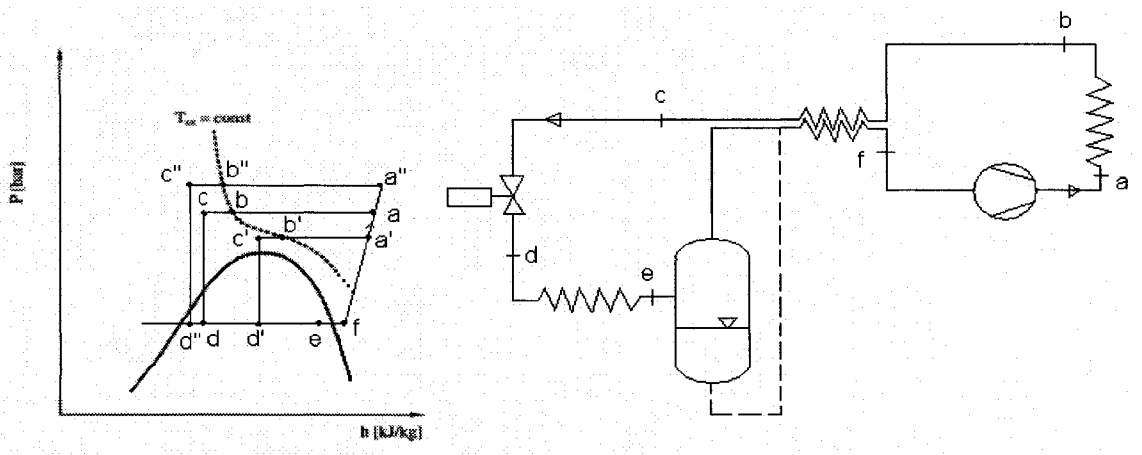

Fig. 3.10 Pressure enthalpy diagram and flow circuit of the transcritical cycle.

The flow circuit and the thermodynamic cycle of the laboratory prototype system are shown in Fig. 3.10, in this system the high-side pressure is regulated by the expansion valve. Varying the momentary refrigerant charge in this part of the circuit can regulate the high–side pressure; this is obtained by adjusting the expansion valve. A reduction in the expansion valve opening causes a temporary reduction in the valve mass flow rate and refrigerant flow to the accumulator, and gives refrigerant accumulation in the high side, causes the pressure to rise and the capacity to increase. This is shown in Fig. 3.10 as the cycle changes from (a b c d e f) to (a″ b″ c″ d″ e f). Conversely, an increase of the expansion valve opening reduces the high-side charge, pressure and capacity, as shown in Fig. 3.10 by cycle (a′ b′ c′ d′ e f). The excess high-side charge is accumulated as liquid in the accumulator. A small liquid flow is bled from the accumulator (dashed line) in order to return oil to the compressor and to provide an over feed of the evaporator (Lorentzen and Pettersen 1992).

CHAPTER 4

4. SYSTEM DESIGN AND EXPERIMENTAL SETUP

The transcritical carbon dioxide refrigeration system that is constructed in Room B05 Essex Hall at the University of Windsor is similar to the automotive air conditioning system; the steps of construction works are listed below:

1. Design the system and produce the design drawing, the system capacity was designed to 4 kW and to suit the existing facilities available in the university.
2. Searching for the components and tubing, select them and obtain prices.
3. Purchase the components.
4. Fabrication of the components in the technical support center of the University of Windsor, this work includes fabrication of gas cooler water tank and evaporator test chamber in addition to other works.
5. Installation of the system and thermal insulation work.
6. Checking, verification and hydraulic pressure test.
7. Troubleshooting.
8. Instruments installation: Eleven numbers of Resistance temperature detectors (RTDs) of insert and surface mounted types were installed to measure the temperatures of the refrigerant in the circuit, two pressure transducers were installed to measure the refrigerant pressure in the suction and discharge lines, a mass flow meter of coriolis type was installed to measure the mass flow rate of the refrigerant in the circuit, a pitot tube is used to measure the air velocity upstream the evaporator, and forty numbers of thermocouples type (T) were fixed to measure the temperatures of refrigerant, air and cooling water of gas cooler.
9. Data reduction: All data is collected with National Instruments (NI) data acquisition system (DAS) and lab view software. The (DAS) consists of an input/output card installed inside the PC, chassis SCXI-1000; two modules type SCXI-1102 and one module type SCXI-1581. Each instrument was assigned to a certain channel, and its signal was tested before connection to its channel in the terminal block. All instruments were connected into the channels in the terminal

blocks that are connected to the modules in the chassis. Virtual instruments were built for temperature and voltage measurements.

4.1 Closed loop Thermal Wind Tunnel

Fig. 4.1 below shows a schematic of the experimental setup with the refrigeration circuit. The experimental facility comprises a thermal closed loop wind tunnel and CO_2 transcritical refrigeration system. The test facilities have been designed to determine system performance of refrigerant side, airside and waterside. The details of the transcritical carbon dioxide system are described bellow in section 4.2. The wind tunnel is located in Room B05 Essex Hall at the University of Windsor; it is used to provide the thermal load on the evaporator. Fig. 4.4 shows the wind tunnel, it is 5440 mm (214 inch) long, 750 mm (30 inch) wide, and 1640 mm (65 inch) high with a contraction ratio of 6.25. The air is forced to flow inside the wind tunnel by means of an air blower, which is driven by an electrically powered hydraulic pump. The air velocity is controlled manually by turning a needle valve attached to the hydraulic pump. The system is capable of producing the air velocity of up to 30 m/s without any obstruction.

The wind tunnel has a water to air cross flow heat exchanger (shown in Fig. 4.5), it is used to provide a thermal load for the evaporator, the temperature of the circulated air in the wind tunnel is controlled by circulating hot water in the heat exchanger, the air temperature can be increased up to 40°C depending on the inlet temperature of the supply water to the heat exchanger. A gap in the wind tunnel is provided for the evaporator chamber, the evaporator chamber is made of a polycarbonate sheet and provided with a number of holes for instruments insertion to measure air temperature, velocity and pressure drop.

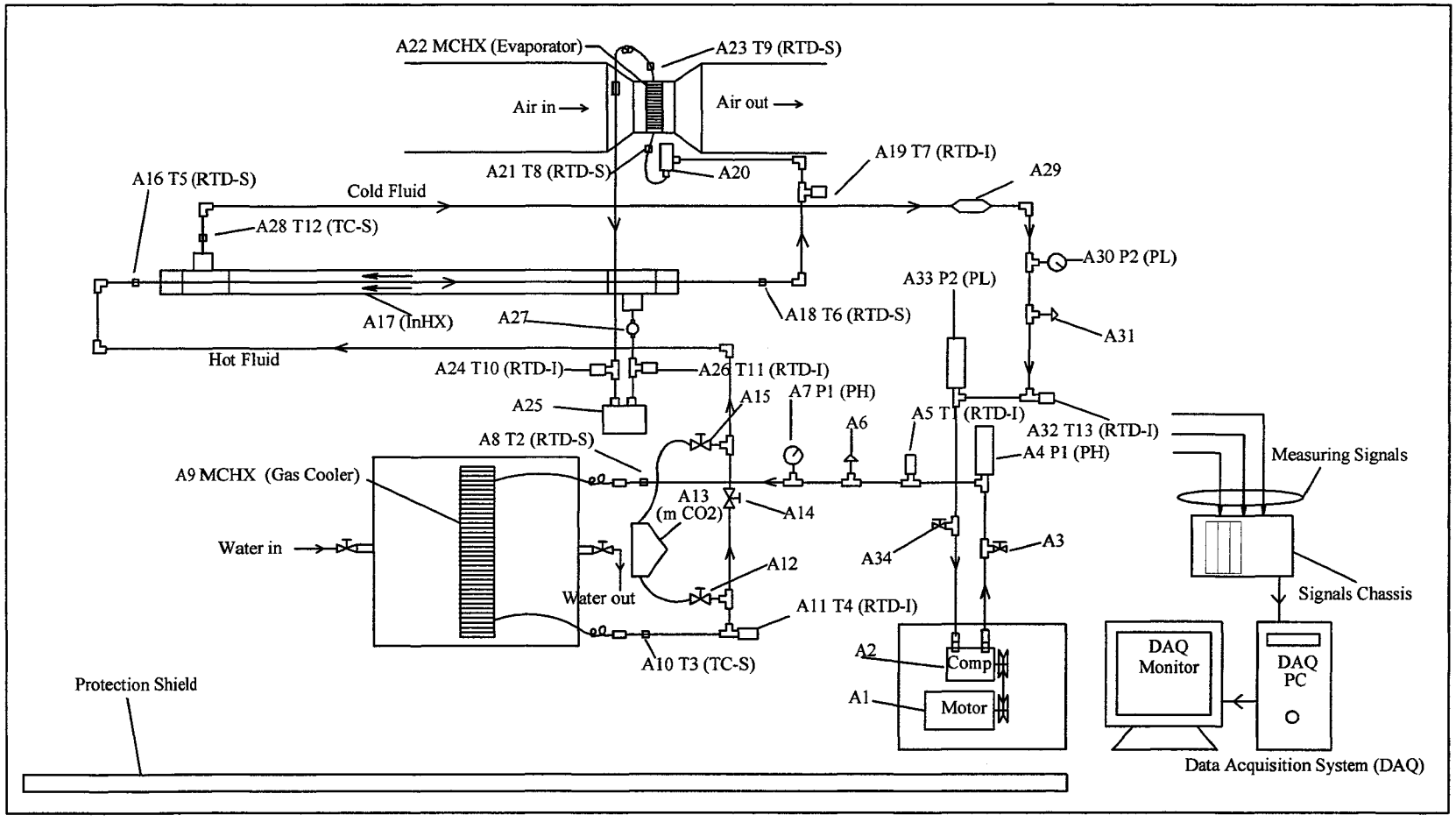

Fig. 4.1 Schematic of experimental setup for transcritical CO2 air conditioning test bench system

Table 4.1 Descriptions of Components & Measuring Sensors
According to the System Schematic
Figure 4.1 (Experiment Sec. A – CO_2 Circuit)

Component and Measuring Sensor	Measuring Parameter	Measuring or Sensor Symbol	Descriptions of the Components and/or Measuring Sensors or Devices
A1	-	-	Electric Motor to run the Compressor of CO_2 Refrigeration System
A2			Compressor of the CO_2 Refrigeration System
A3			Discharge or high pressure line service valve (to vacuum the system)
A4	Pressure (abs.)	P1 or P_H	Discharge or high pressure side Insert Absolute Pressure Transducer (PressTDA) – measures CO_2 refrigerant Pressure at Compressor exit
A5	Temperature	T1	Discharge or high pressure side Insert Temperature Sensor (RTD-I) – measures hot CO_2 refrigerant Temperature at Compressor exit
A6			Discharge /high pressure side safety valve – releases excess pressure
A7	Pressure (abs.)	P1 or P_H	Discharge or high pressure side Pressure Gage – displays hot CO_2 refrigerant Pressure after Compressor exit & before Gas cooler inlet
A8	Temperature	T2	Discharge / high pressure side Surface Temperature Sensor (RTD-S) on hot CO_2 tube – measures tube surface Temp. at Gas cooler inlet
A9			Microchannel Heat Exchanger used as CO_2 Gas cooler (MCHXGc)
A10	Temperature	T3	High pressure side Surface Temperature Sensor (TC-S) on hot CO_2 tube surface – measures tube surface Temp. at Gas cooler exit
A11	Temperature	T4	High pressure side Insert Temperature Sensor (RTD-I) – measures hot CO_2 refrigerant Temperature after Gas cooler exit and before Internal Heat Exchanger (InHX) inner pipe inlet (i.e. hot fluid inlet)
A12			Flow control valve at Mass Flow Meter (MFM) inlet
A13	Mass flow rate (CO_2)	$\dot{m}_{CO2}$	Coriolis Mass Flow Meter after Gas cooler exit – measures CO_2 refrigerant mass flow rate through the syste
A14			Flow control valve for bypassing the Mass Flow Meter (MFM) path
A15			Flow control valve at Mass Flow Meter (MFM) exit

Component and Measuring Sensor	Measuring Parameter	Measuring or Sensor Symbol	Descriptions of the Components and/or Measuring Sensors or Devices
A16	Temperature	T5	High pressure side Surface Temperature Sensor (RTD-S) on hot CO_2 tube surface – measures tube surface Temp. at InHX inner pipe inlet (i.e. hot fluid inlet)
A17			Internal Heat Exchanger (InHX) – Double pipe shell-and-tube type
A18	Temperature	T6	High pressure side Surface Temperature Sensor (RTD-S) on hot CO_2 tube surface – measures tube surface Temp. at InHX inner pipe exit (i.e. hot fluid exit)
A19	Temperature	T7	High pressure side Insert Temperature Sensor (RTD-I) – measures hot CO_2 refrigerant Temp. after InHX inner pipe exit (hot fluid exit) and before the Expansion valve inlet
A20			Expansion valve before Evaporator inlet – expands CO_2 to lower pressure and temperature
A21	Temperature	T8	Low pressure side Surface Temperature Sensor (RTD-S) on cold CO_2 tube surface – measures tube surface Temp. at Evaporator inlet
A22			Microchannel Heat Exchanger used as CO_2 Evaporator (MCHXEv)
A23	Temperature	T9	Low pressure side Surface Temperature Sensor (RTD-S) on cold CO_2 tube surface – measures tube surface Temp. at Evaporator exit
A24	Temperature	T10	Low pressure side Insert Temperature Sensor (RTD-I) – measures cold CO_2 refrigerant Temp. after Evaporator exit and before the Accumulator inlet
A25			Accumulator
A26	Temperature	T11	Low pressure side Insert Temperature Sensor (RTD-I) – measures cold CO_2 refrigerant Temp. after Accumulator exit and before InHX outer pipe / annuli inlet (i.e. cold fluid inlet)
A27			Sight glass to watch /visualize the state of cold CO_2 refrigerant flow
A28	Temperature	T12	Suction or low pressure side Surface Temperature Sensor (TC-S) on cold CO_2 tube surface – measures tube surface Temp. at InHX outer pipe / annuli exit (i.e. cold fluid exit)

Component and Measuring Sensor	Measuring Parameter	Measuring or Sensor Symbol	Descriptions of the Components and/or Measuring Sensors or Devices
A29			Suction or low pressure side CO_2 Refrigerant Filter installed on cold fluid line after InHX and before Compressor
A30	Pressure (abs.)	P2 or P_L	Suction or low pressure side Pressure Gage – displays cold CO_2 refrigerant Pressure after InHX outer pipe / annuli exit (cold fluid exit) and before Compressor inlet
A31.	-	-	Suction / low pressure side safety valve – releases excess pressure
A32.	Temperature	T13	Suction or low pressure side Insert Temperature Sensor (RTD-I) – measures cold CO_2 refrigerant Temperature at Compressor inlet
A33.	Pressure (abs.)	P2 or P_L	Suction or low pressure side Insert Absolute Pressure Transducer (PressTDA) – measures CO_2 refrigerant Pressure at Compressor exit
A34.			Suction or low pressure line service valve (to charge the system)

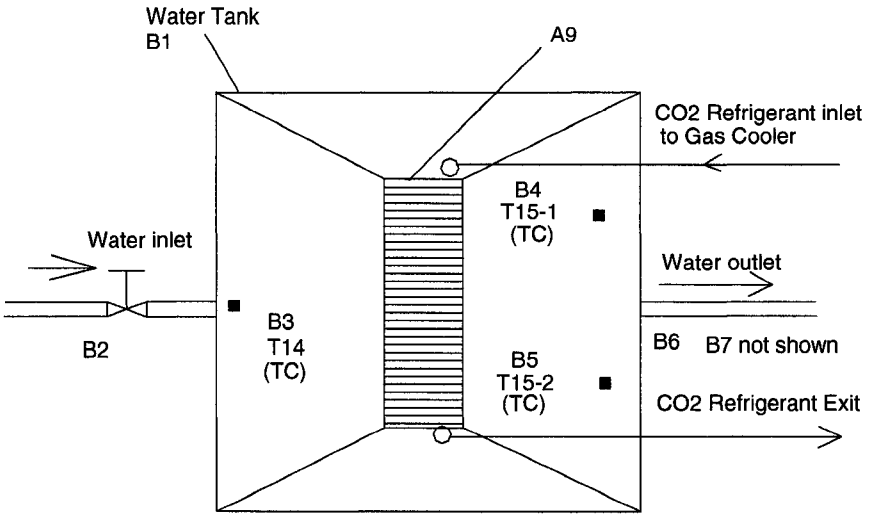

Fig. 4.2 Schematic of gas cooler

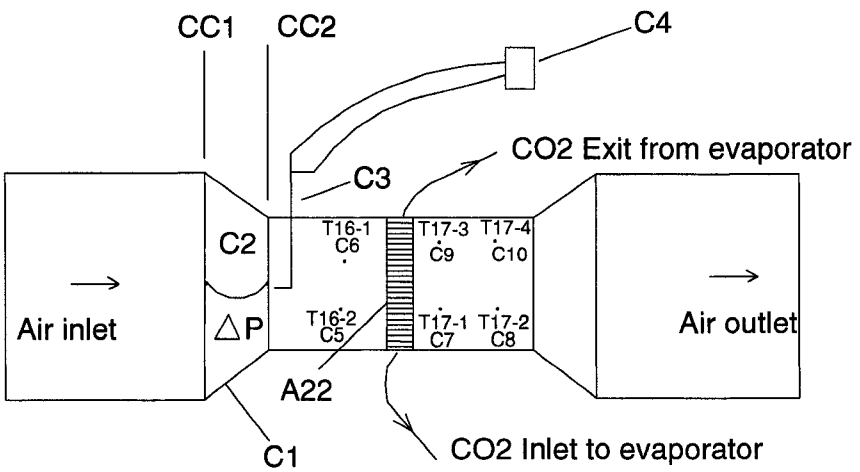

Fig. 4.3 Schematic of evaporator section in wind tunnel

Table 4.2 Descriptions of Components & Measuring Sensors
According to the System Schematic
Figures 4.2 & 4.3

Component and Measuring Sensor	Measuring Parameter	Measuring or Sensor Symbol	Descriptions of the Components and/or Measuring Sensors or Devices
B1.	-	-	Water tunnel (open circuit) for Gas cooler heat transfer
B2.	-	-	Control valve at Water tunnel inlet or upstream – controls water flow through the Gas cooler
B3.	Temperature	T14	Temperature Sensor (TC) – measures inlet or upstream temperature of water flowing through the Gas cooler
B4.	Temperature	T15-1	Temperature Sensor (TC) – measures exit or downstream temp. of water flowing through Gas cooler (at CO_2 inlet side of Gas cooler)
B5.	Temperature	T15-2	Temperature Sensor (TC) – measures exit or downstream temp. of water flowing through Gas cooler (at CO_2 exit side of Gas cooler)
B6.	-	-	Control valve at Water tunnel exit or downstream – controls discharge of water from the Water tunnel after Gas cooler
B7.	Mass flow rate (water)	$\dot{m}_{H2O}$	Arrangements for measuring the water mass flow rate through Gas cooler – measures $\dot{m}_{H2O}$ at Water tunnel discharge side (Not shown)
C1.	-	-	Thermal Wind tunnel (closed circuit) for Evaporator heat transfer
C2.	Pressure difference	$\Delta P_{contraction}$ (for $\dot{m}_{Air}$)	Airflow pressure drop (ΔP) measurement across Wind tunnel contraction using Digital Manometer – to estimate air mass flow rate
C3.	Pressure difference	ΔP_{Pitot} (for V_{Air})	Pitot static tube to measure Wind tunnel air velocity (via total & static pressure difference, ΔP_{Pitot}) upstream or inlet to the Evaporator
C4.	Pressure difference	ΔP_{Pitot} (for V_{Air})	Differential Pressure Transducer (PressTDD) connected to Pitot static tube to record total & static pressure difference, ΔP_{Pitot} of Wind tunnel air upstream or inlet to the Evaporator

Component and Measuring Sensor	Measuring Parameter	Measuring or Sensor Symbol	Descriptions of the Components and/or Measuring Sensors or Devices
C5.	Temperature	T16-1	Temperature Sensor (TC) – measures Wind tunnel air temperature inlet or upstream to the Evaporator (at CO_2 inlet side of Evaporator)
C6.	Temperature	T16-2	Temperature Sensor (TC) – measures Wind tunnel air temperature inlet or upstream to the Evaporator (at CO_2 exit side of Evaporator)
C7.	Temperature	T17-1	Temperature Sensor (TC) – measures Wind tunnel air temperature immediate exit / downstream to the Evaporator (at CO_2 inlet side of the Evaporator)
C8.	Temperature	T17-2	Temperature Sensor (TC) – measures Wind tunnel air temperature far exit / downstream to the Evaporator (at CO2 inlet side of the Evaporator)
C9.	Temperature	T17-3	Temperature Sensor (TC) – measures Wind tunnel air temperature immediate exit / downstream to the Evaporator (at CO_2 exit side of the Evaporator)
C10.	Temperature	T17-4	Temperature Sensor (TC) – measures Wind tunnel air temperature at far exit / downstream to the Evaporator (at CO_2 exit side of the Evaporator)

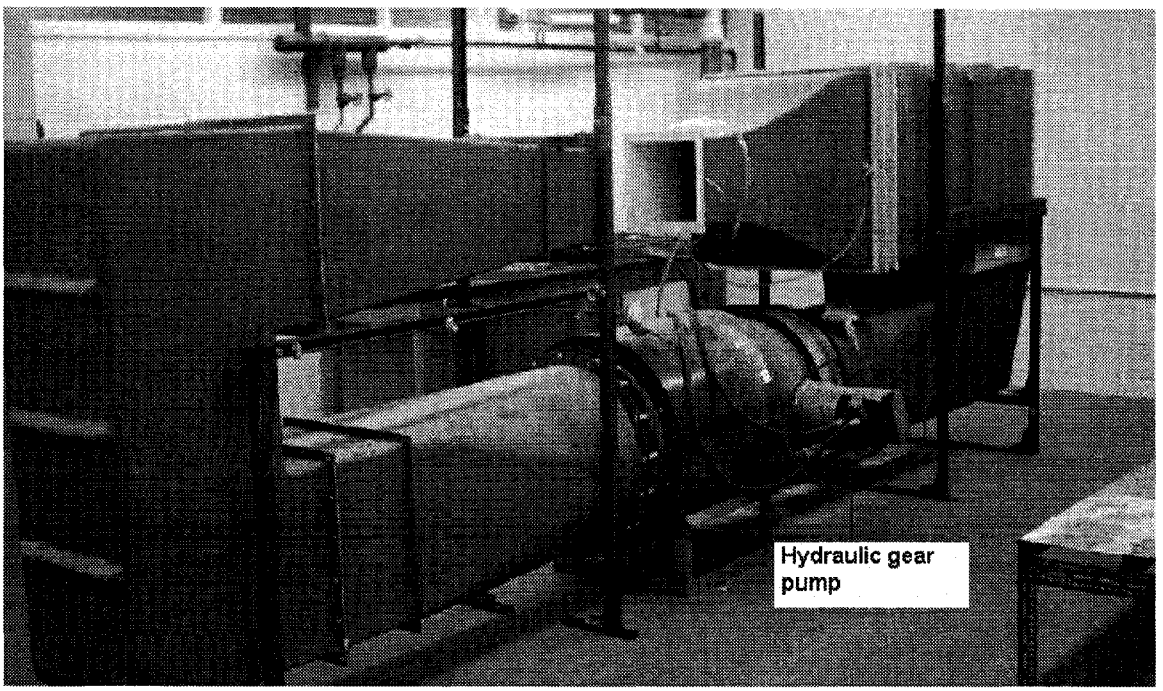

Fig. 4.4 Wind tunnel assembly.

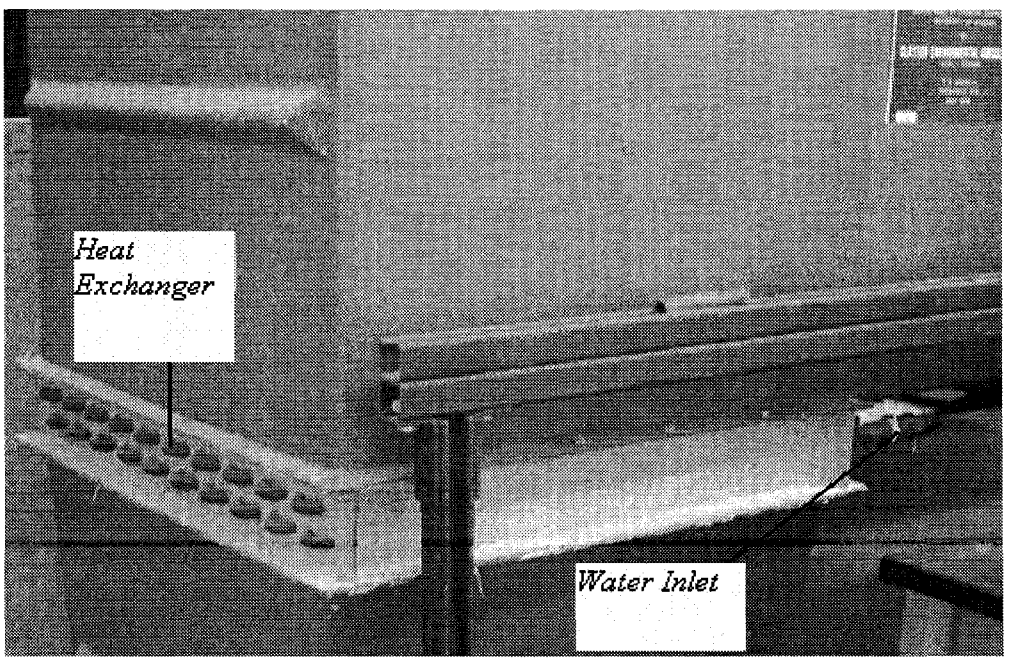

Fig. 4.5 Heat exchanger of wind tunnel

4.2 System Components

The system components used in this experimental setup are: a drive motor, a compressor, a gas cooler, an electrical expansion valve, an evaporator, an internal heat exchanger and an accumulator.

4.2.1 Compressor

The compressor is shown in Fig. 4.6, it is a positive displacement reciprocating compressor, swash plate type, belt driven, and its volume displacement is 29 cm^3, and volumetric efficiency ranges from 88% to 78% (based on test condition). It works with a minimum suction pressure of 30 bar and it discharge pressure is 140 bar, The maximum rotation speed is 9500 rpm, recommended maximum capacity tests till 2400 rpm. The compressor is activated by an electromagnetic clutch that can engage or disengage the compressor pulley according to commands from A/C system.

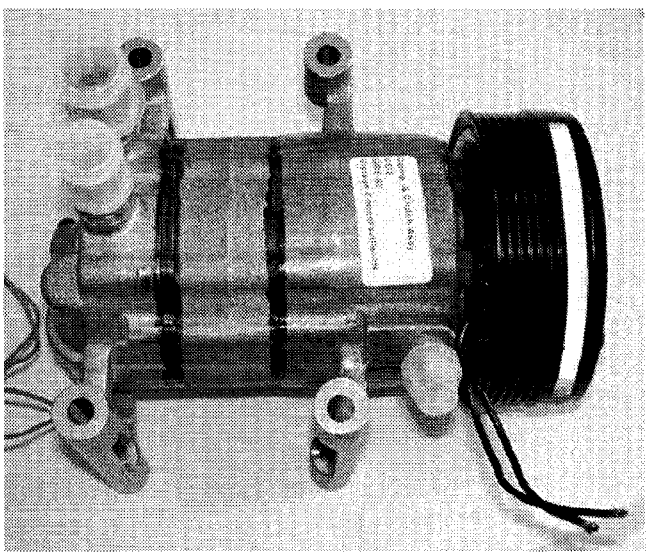

Fig. 4.6 The compressor.

The compressor is driven by a variable speed electric motor via a five groves belt, a mobile motor cart has been arranged to fix the compressor on it and drive it. Fig. 4.7 shows the motor cart, it consists of:

- Isolator switch: 20 amp on-off isolator switch to isolate the whole system from incoming power.
- Main switch: 3 phase, 20 amps, 208 volt ac main switch with 40 amp, 208 volt overload magnetic coil to protect motor from overloading.
- Off-On switch: to start and stop the motor.
- Variable frequency drive: to control the motor speed within the range from 0 to 1750 rpm. The rpm of the motor can be calculated from the following equation:

$$Srpm = \frac{120 \times f}{N}$$

$Srpm$ = synchronous revolution per minute.

120 = constant

f = supply frequency (in cycles/s).

N = number of poles, the used motor has 4 poles.

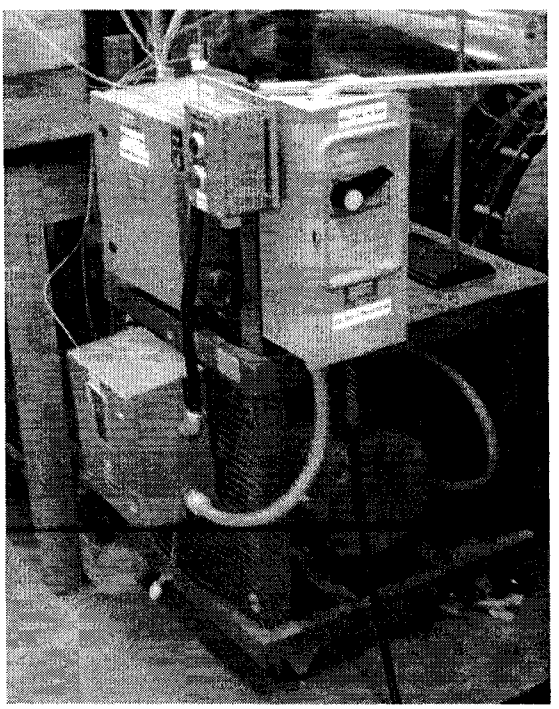

Fig.4.7 The drive motor cart.

Table. 4.3 Specification of electric motor

Power	7.5 (hp)
Rpm	1750
Phase	3
Voltage	208 volt ac

4.2.2 Gas Cooler

Water cooled gas cooler is used in this experiment, the gas cooler is a microchannel heat exchanger fixed in a square shape tank as shown in Fig 4.8. The tank is fabricated in the machine shop of the University of Windsor; it is (800mm) long, (700mm) wide and (600mm) high, made of aluminum, it has two openings for inlet and outlet of water, there are separators, so the incoming water does not mix with the outgoing water, all delivered water has to pass through the heat exchanger.

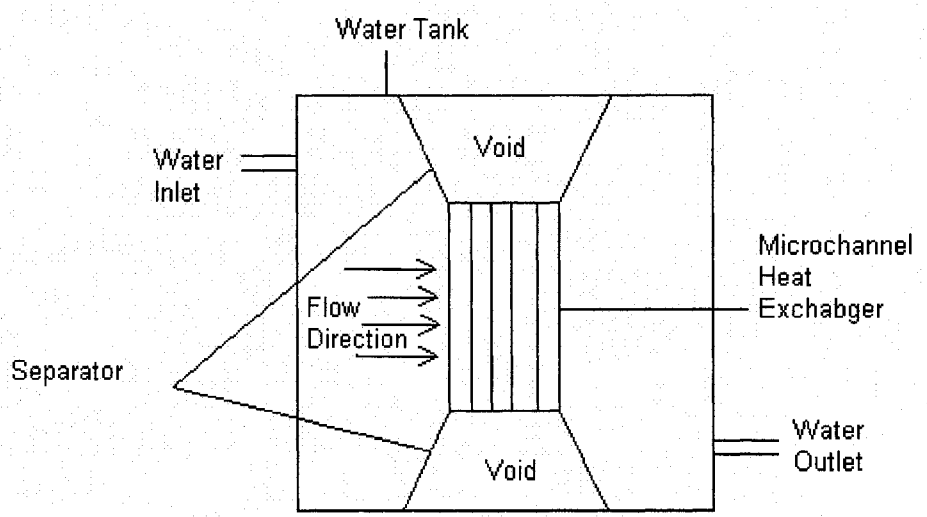

Fig. 4.8 Schematic of water-cooled gas cooler.

Fig. 4.9 shows the microchannel heat exchanger, it consists of three sections, each section has one tube with five passes, and the tube has 68 ports of 1 mm internal diameter. The heat exchanger is 300 mm wide, 300 mm long and 100 mm deep.

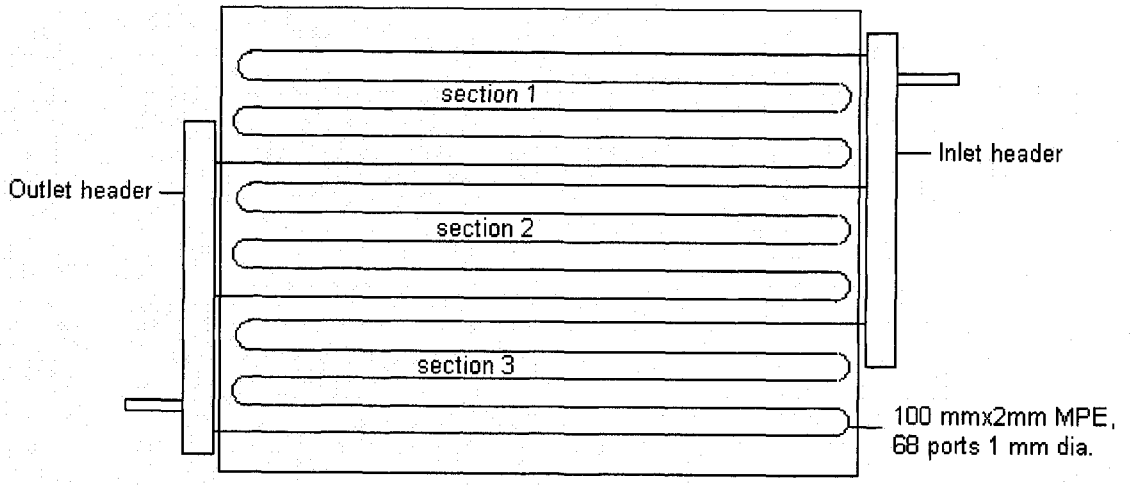

Fig. 4.9 Schematic of gas cooler.

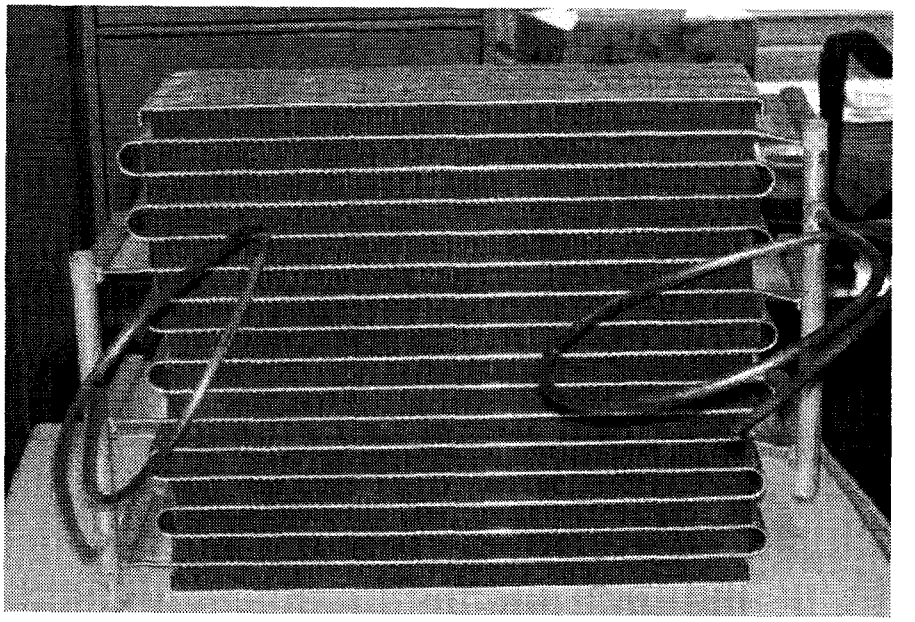

Fig. 4.10 The gas cooler before fixing inside water tank

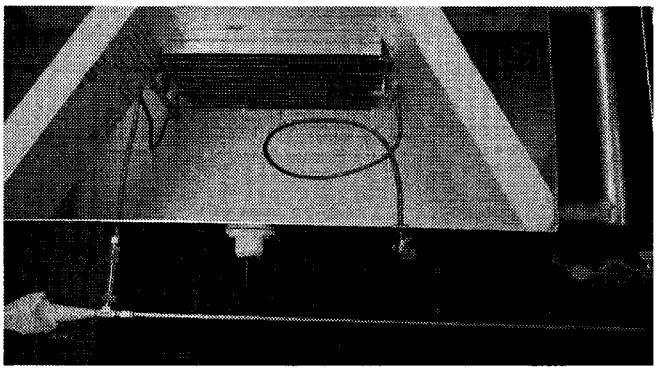

Fig. 4.11 The gas cooler after fixing inside water tank

Table. 4.4 Gas cooler data

Type	Gas to water cross flow heat exchanger
Material	Extruded aluminium
Capacity	4 kW
Size	300 mm x 300 mm x 100 mm
Face area (m^2)	0.0874
Header	½ inch ID
Tube diameter OD (m)	0.002
Tube diameter ID (m)	0.001
Number of ports per tube	68
Number of circuits	3
Number of passes per circuit	5
Refrigerant side area (m^2)	0.96084
Inlet temperature	0 to 200 °C

4.2.3 Evaporator

The evaporator is made of aluminum; the core is made of extruded microchannel tubes with louvered fins. The evaporator is fixed in a test chamber has a cross section of 300mm x 300mm, which is fixed in a gap provided for that purpose in the wind tunnel. Fig. 4.12 shows the evaporator after fixing in the test chamber. Several opening are provided in the test chamber to enable air velocity, temperatures and pressure drop measurement.

Table. 4.5 Evaporator data

Type	Gas to air cross flow heat exchanger
Material	Extruded aluminium
Capacity	4 kW
Size	300 mm x 300 mm x 100 mm
Face area (m^2)	0.0874
Header	½ inch ID
Tube diameter OD (m)	0.002
Tube diameter ID (m)	0.001
Number of ports per circuit	68
Number of circuits	3
Number of passes per circuit	5
Air side surface (m^2)	16.634
Air free area (m^2)	0.07348
Refrigerant side area (m^2)	0.96084
Refrigerant Inlet temperature	0 to 200 °C
Refrigerant mass flow rate	0.02-0.06 kg/s
Air face velocity	10 m/s
Air flow rate	0.5-1.1 kg/s
Air inlet temperature	32 °C
Air side pressure drop	80 Pa

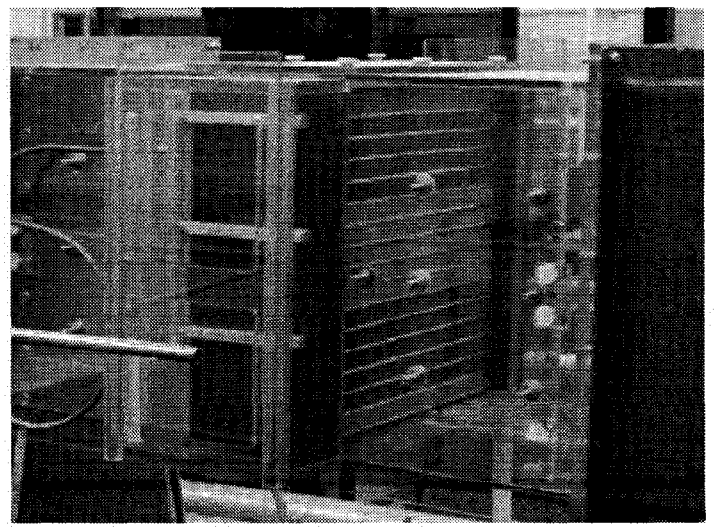

Fig. 4.12 Evaporator after fixing in the test chamber

4.2.4 Expansion Valve

The expansion valve is a 12V DC, solenoid operated, angle type valve.

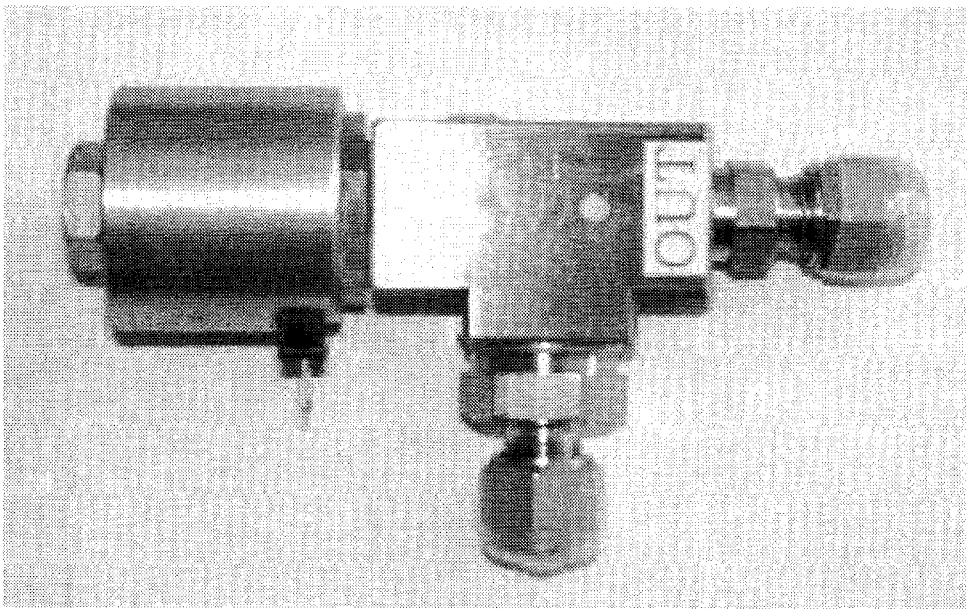

Fig. 4.13 Solenoid expansion valve

4.2.5 Accumulator

The accumulator shown in Fig. 4.14 is a cylindrical vessel has a capacity of 2130 cm^3. It is installed at the exit of the evaporator. It has been designed to withstand the high operating pressure; its operating pressure is 17 MPa. Its specification is given in table 4.6 below.

Table. 4.6 Accumulator data

Material	Carbon steel
Connection fitting	6 mm (¼ inch) MNPT
Inlet temperature	-5 to 20 °C
Outlet temperature	-5 to 20 °C
Working pressure	17 MPa
Mass flow rate	0.02 to 0.06 kg/s

Fig. 4.14 Accumulator

4.2.6 Internal Heat Exchanger

The internal heat exchanger is a double pipe heat exchanger made of two concentric stainless steel pipes Fig. 4.15(a,b) shows it's identical cross sections. It has been fabricated manually in the laboratory of the University of Windsor. The outside diameter of the inner tube is 9.52 mm (3/8 inch); it has a wall thickness of 1.65 mm (0.065 inch). The outside diameter of the outer tube is 19 mm (¾ inch); it has a wall thickness of 1.65 mm (0.065 inch). The length of the inner tube is 1650 mm, and the length of the outer tube is 1359 mm, the inner tube is placed inside the outer tube and fixed at both ends with run through tees as shown in the Fig. 4.15. The hot supercritical fluid flows in the internal tube while the cold low-density fluid flows in the outer tube, the outer surface of the annulus is thermally insulated and heat transfer to the surrounding assumed to be zero.

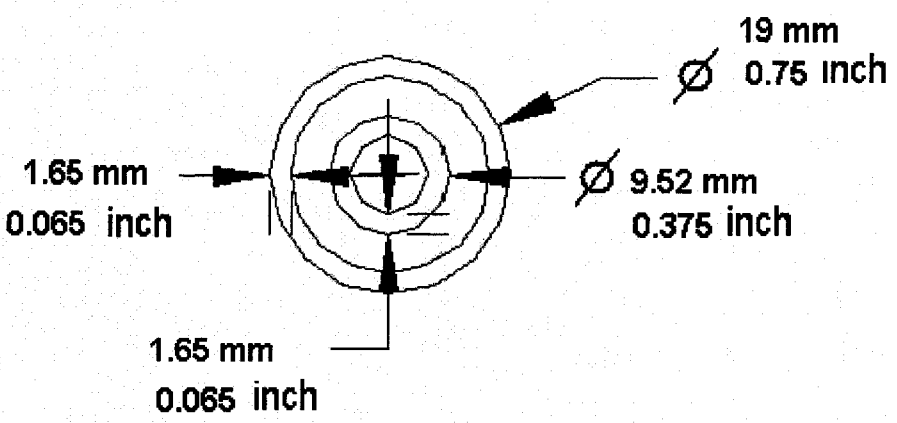

(a) Cross section of internal heat exchanger

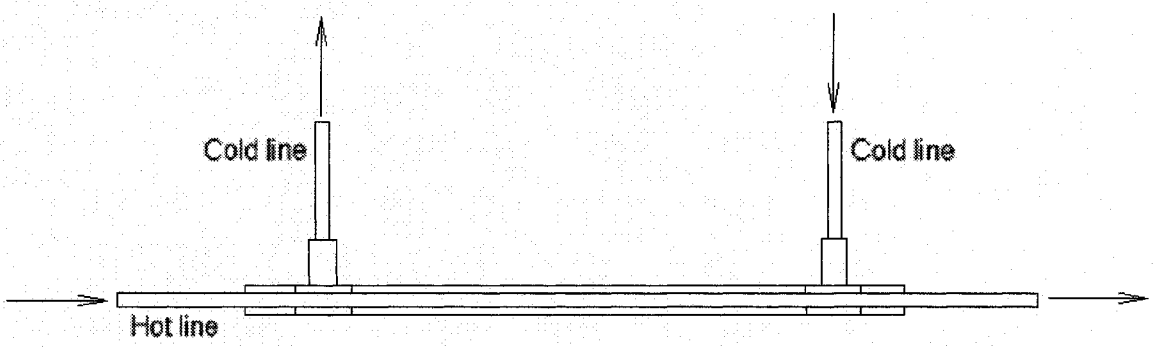

(b) Longitudinal cross section of internal heat exchanger

Fig. 4.15 Cross sections of internal heat exchangers

4.2.7 Tubing, Fittings and Flexible Hoses

The tubing, fittings, valves, pressure gauges and flexible hoses are manufactured by (Swagelok). The tubing are stainless steel, the low pressure side tubing has an outside diameter of 9.52 mm (3/8 inch) and a wall thickness of 0.89 mm (0.035 inch), it can be used in operating pressure up to 210 bar, and the high pressure side tubing has an outside diameter of 9.52 mm (3/8 inch) and a wall thickness of 1.65 mm (0.065 inch), it can be used in operating pressure up to 421 bar.

The allowable working pressure for the fittings is from 330 bar to 496 bar, it depends on the type and size of the fitting. Flexible hoses are used to absorb the movement of the compressor during operation, for the low pressure side type FM6 is used, it is designed for working pressure up to 136 bar, for the high pressure side type FM4 is used, it is designed for working pressure up to 210 bar.

4.2.8 Valves

A service valve is provided on each of the suction and discharge sides of the compressor, they are used for the discharging and filling of the system. These valves have a maximum operating pressure of 17 MPa. Three isolating valves are provided for the isolation of the mass flow meter, these valves enable to run the system with/without a mass flow meter. They have an operating pressure of 17 MPa. The system has low and high-pressure safety relief valves. The valve on the low-pressure side was set at 5 MPa and the valve on the high-pressure side was set at 12 MPa. These valves will open and relief refrigerant pressure to the atmosphere when the pressure in the line exceeds the set pressure of the valve at that line.

4.2.9 Filter Dryer

A filter dryer is installed in the suction line to remove the solid contaminants in the piping following installation, and to protect the system from excessive moisture, dirt and acids.

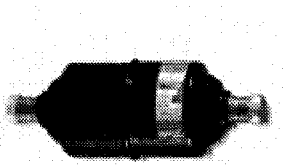

Fig. 4.16 Suction line filter dryer

4.2.10 Instrumentation

The instrumentation was designed to measure airside, waterside and refrigerant side properties. There are basically three types of measurements necessary to obtain the required data to calculate and evaluate the performance of the CO_2 cycle. These measurements are temperatures, pressures and mass flow rates. All data from instruments are collected by data acquisition system.

- **Temperature Measurement:**

The refrigerant temperatures at various locations in the system are measured by Resistance temperature detectors (RTDs), the (RTD) is an electrical resistor, as temperature changes its resistance changes. RTD's resistance increases as the temperature increases. High pressure (RTDs) plug sensors made by Omega were used in this work; its 304SS sheath has a 6.0 mm diameter probe that extends 12.7 mm from 6.0 mm NPT pipe plug. Its pressure rating is 166 bars and maximum temperature rating is 230°C. Surface RTDs are used as well to measure the refrigerant temperature; they are small and flexible sensors. The insert and surface mounted types RTDs are shown in Fig 4.16 (a,b) respectively.

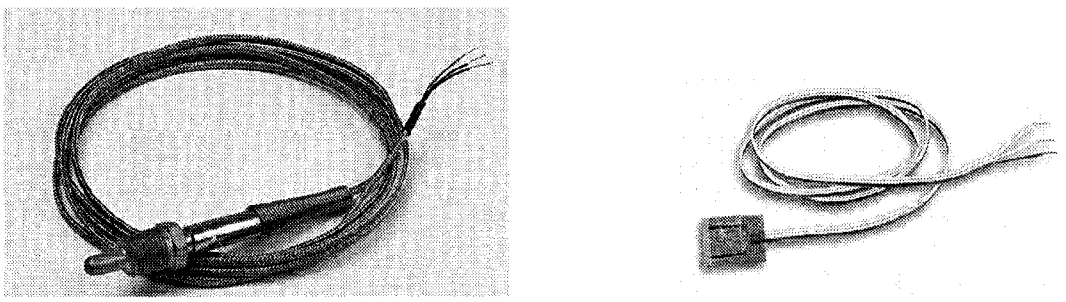

a- Insert type RTD b- Surface mounted RTD

Fig. 4.17 RTDs insert and surface types

In addition to the RTDs thermocouples type T are used as well to measure the water and air temperatures.

- **Pressure Measurement:**

Two Pressure Transducers made by Omega are used to measure the refrigerant pressures at the compressor suction and discharge sides. They are hermetically sealed, all stainless steel construction, high accuracy, and mill volts output. On the compressor suction side PX35DO 1KGV is used, its pressure ranting is from 0 to 66 bars, and on the compressor discharge side PX35DO 3KGV is used, its pressure rating is from 0 to 200 bars, controller units are used to provided an voltage signal to excite the pressure transducers, and to receive the out put signals of the pressure transducers and convert them into pressure values.

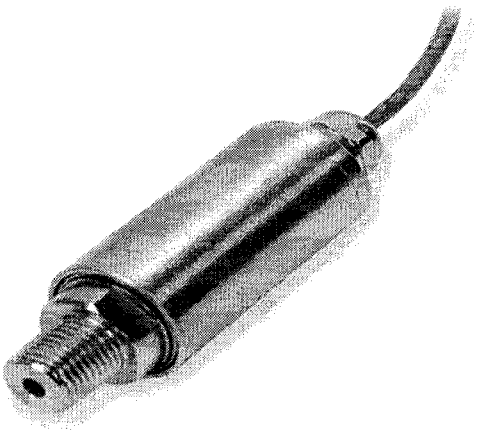

Fig. 4.18 Pressure transducer

- **Refrigerant Mass Flow Rate Measurement:**

The refrigerant mass flow rate is measured with a coriolis mass flow meter installed in the system; it has a range from 0 to 50 kg/min.

4.3 Experimental Procedure and Sample Calculations

An electrical vacuum pump was connected to the system through the service valve to extract the air inside the system before charging, and then the system was charged by an initial amount of carbon dioxide before operating, the CO_2 used to charge the system had a purity of 99.96. Meanwhile the air blower of the wind tunnel was put on, and hot water was circulated in the wind tunnel heat exchanger (to adjust the water temperature) for 30 minutes to achieve steady state condition, the air velocity and temperature were kept constant at 3.5 m/s and 31.5°C respectively. The water mass flow rate and its temperature through the gas cooler tank were adjusted to 0.2 kg/s and 45.4°C respectively. Then the speed of the compressor was adjusted to 1100 rpm through a variable frequency drive and the charging procedure continued till the discharge pressure of the compressor exceeded the critical pressure. Different operating conditions were applied during system operation; every component was tested for proper performance. A coriolis mass flow meter was used with a display unit to measure the refrigerant mass flow rate during test run. Readings were collected by the data acquisition system for every operating condition, and one set of data was used for drawing the refrigeration cycle as shown in Fig. 4.19 below.

- **Sample Calculations**

The system was tested for different operating conditions, the temperature and flow rate of air and water were changed frequently, and the compressor rpm was adjusted at each condition to achieve the highest discharge pressure. At each operating condition the system was kept running for 30 minutes to reach steady state. One set of data from one operating condition was selected to show a sample calculation. Table 4.7 below shows the sample of data used in the calculations.

Table 4.7 Sample of data representing one operating condition

Refrigerant temperature entering gas cooler	116.6°C
Refrigerant temperature leaving gas cooler	47.4°C
Refrigerant temperature entering ihx hot	47.1°C
Refrigerant temperature leaving ihx hot	44.7°C
Refrigerant temperature before expansion valve	45.9°C
Refrigerant temperature after expansion valve	9.5°C
Refrigerant temperature after evaporator	27.1°C
Refrigerant temperature entering ihx cold	27.1°C
Refrigerant temperature leaving ihx cold	32.6°C
Refrigerant temperature entering compressor	33.6°C
Water temperature entering gas cooler	40.0°C
Water temperature leaving gas cooler	45.4°C
Air temperature entering evaporator	31.5°C
Air temperature leaving evaporator	24.9°C
Compressor speed	1078 rpm
Refrigerant mass flow rate	0.0282 kg/s
Compressor current	17.2 amp
Compressor discharge pressure	94.7 bar
Compressor suction pressure	38.4 bar

Table 4.8 below shows the refrigerant enthalpy at different points in the system which were used to determine the cooling capacity and coefficient of performance of the refrigeration cycle.

Table 4.8 Refrigerant properties throughout the refrigeration cycle

Enthalpy of refrigerant entering gas cooler	24.96 kJ/kg
Enthalpy of refrigerant leaving gas cooler	-119.5 kJ/kg
Enthalpy of refrigerant entering IHX hot	-121.4 kJ/kg
Enthalpy of refrigerant leaving IHX hot	-129.5 kJ/kg
Enthalpy of refrigerant leaving evaporator	-50.58 kJ/kg
Enthalpy of refrigerant entering IHX cold	-50.64 kJ/kg
Enthalpy of refrigerant leaving IHX cold	-42.41 kJ/kg

- **Evaporator Cooling Capacity**

The refrigerant-side capacity was calculated by the refrigerant mass flow rate and the enthalpy difference between inlet and outlet of evaporator, as stated in the following equation:

$$q_{ev.r} = \dot{m}_r \, (h_{r.ev.o} - h_{r.ev.i}) \qquad (4.1)$$

$\dot{m}_r = 0.0282$ kg/s

$h_{r.ev.i} = -129.5$ [kJ/kg], $h_{r.ev.o} = -50.58$ [kJ/kg]

$q_{ev.r} = 0.0282$ kg/s x (- 50.58 - (- 129.5))

$q_{ev.r} = 2.225$ kJ/s

The airside capacity was determined by the air mass flow rate, specific heat of air *Cp* and the air temperature difference at the inlet and outlet of evaporator. Thus,

$$q_{ev.a} = \dot{m}_a \, . Cp_a \, . \, (T_{a.o} - T_{a.i}) \qquad (4.2)$$

$q_{ev.a} = 0.3015$ kg/s x 1.0067 kJ/kg/K x (24.9098-31.533)

$q_{ev.a} = -2.0103$ kJ/s

There exists an error of 10% between the two heat transfer quantities in evaporator.

- **Gas Cooler Capacity**

The refrigerant-side capacity ($q_{g.r}$) was calculated by the refrigerant mass flow rate and the refrigerant enthalpy difference between inlet and outlet of gas cooler. Thus, the cooling effect ($q_{g.r}$) was calculated using Equation (4.3).

$q_{g.r} = \dot{m}_r$ x ($h_{r.g.o}$ - $h_{r.g.i}$) (4.3)

$q_{g.r}$ = 0.0282 kg/s x (- 119.5- 24.96)

$q_{g.r}$ = - 4.0738 kJ/s

The water side capacity ($q_{g.w}$) was calculated by the water mass flow rate and the water temperature difference between inlet and outlet of gas cooler.

$q_{g.w} = \dot{m}_w \ .Cp_w . (T_{w.o} - T_{w.i})$

$q_{g.w}$ = 0.199 kg/s x 4.183 kJ/kg/K x (45.43- 40.0)

$q_{g.w}$ = 4.521 kJ/s

There exists an error of 10% between the two heat transfer quantities in Gas Cooler as well.

- **Compressor Power**

The compressor power was calculated by using the refrigerant mass flow rate and the enthalpy difference at the suction and discharge lines of the compressor.

$W_{comp} = \dot{m}_r$ x ($h_{r.g.i}$ - $h_{r\ ihx..c.\ o}$) (4.4)

W_{comp} = 0.0282 kg/s x (24.96 – (- 42.41))

W_{comp} = 1.9 kJ/s

- **Coefficient of Performance (COP)**

The coefficient of performance is calculated from the evaporator cooling capacity and the compressor work.

COP = 2.225/ 1.9

COP = 1.17

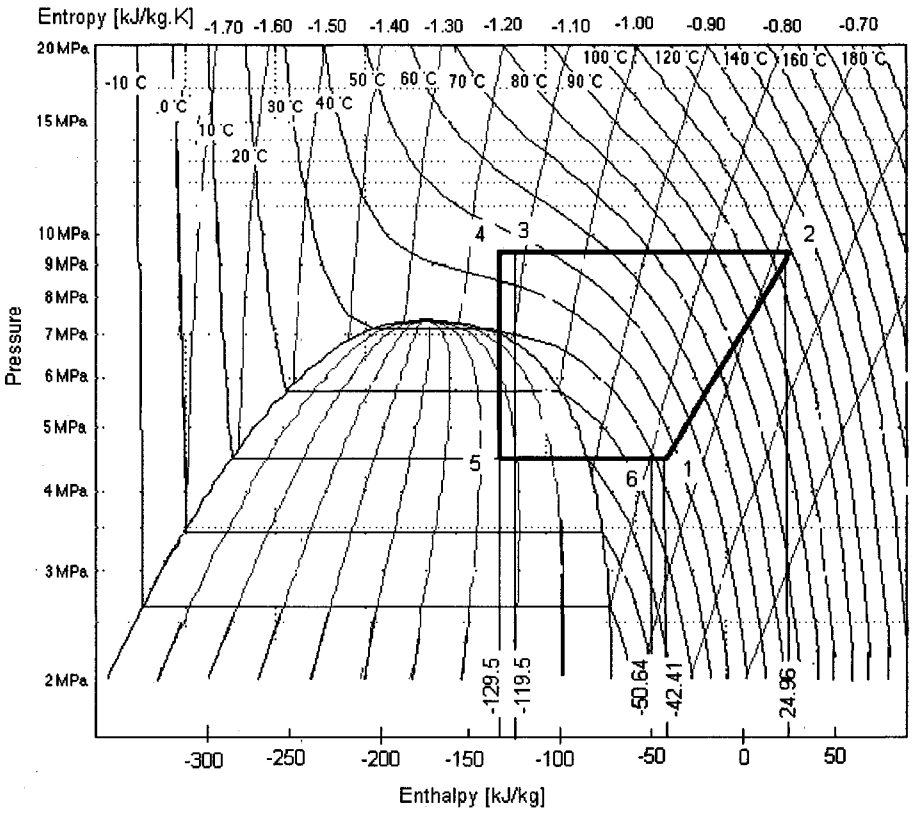

Fig. 4.19 Refrigeration cycle on enthalpy pressure diagram

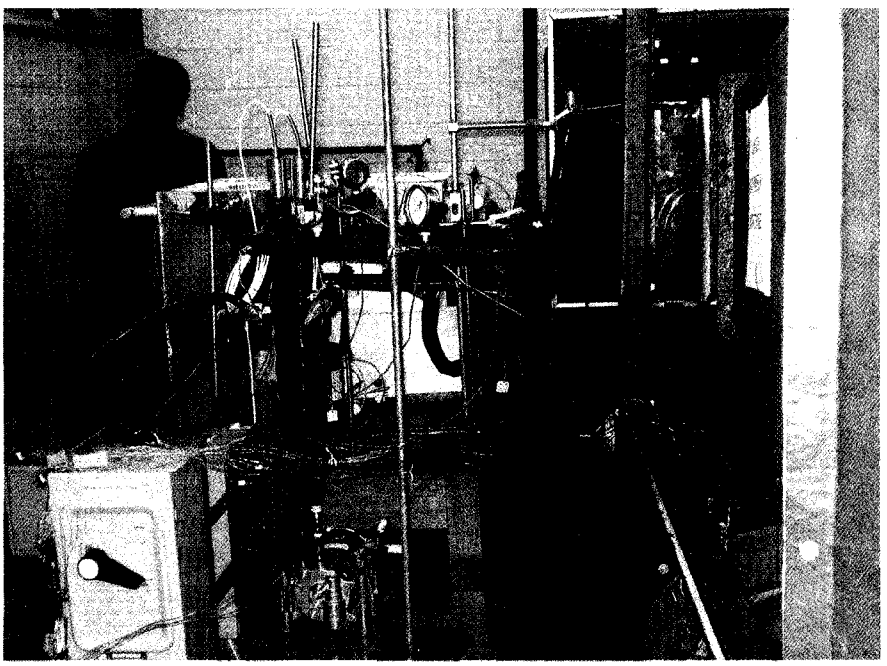

Fig. 4.20 CO2 System after completion

CHAPTER 5

5. CONCLUSIONS AND RECOMMENDATION

5.1 Conclusions

The main objective of this study was to construct and operate a fully instrumented transcritical carbon dioxide refrigeration test bench. The system was constructed and put into operation successfully. Several test runs were carried out for several hours per day for one week. A swash plate compressor and michrochannel evaporator and gas cooler were used in this work. Data acquisition system and instrumentation were installed and operated efficiently. During the test run all components performed properly and responded well to the different operating conditions. The system was charged to raise the compressor discharge pressure above the critical point, the system was operating at 95 bar on the high side pressure and 39 bar at the low side pressure, the compressor compression ratio was 2.5.

5.2 Recommendation

It is important to increase the compressor discharge pressure above 95 bar. In order to improve the system performance, it is required to control the expansion valve precisely, as it was widely opened during the test runs. A comprehensive experimental study on CO_2 flow in microchannel heat exchanger can also be investigated. Furthermore system performance can be studied by mixing another refrigerant with the CO_2 to bring down the high operating pressures.

REFERENCES

Althouse A. D., Thrnquist C. H., and Bracciano A.F.,2003. Modern Refrigeration and Air Conditioning. Goodheart- willcox publisher.

Boewe D. E., McEnaney R. P., Park Y. C., Yin J. M., Bullard C. W., and Hrnjak P. S. 1999. Comprehensive experimental study of subcritical R134a and transcritical R744 refrigeration systems for mobile applications, ACRC reportCR-17 University of Illinois at Urbana- Champaign, Illinois.

Centre for Atmospheric Science. 1980. University of Cambridge. Part1: The History Behind The Ozone Hole. Electronic Source. http://www.atm.ch.cam.ac.uk/tour/part1.

Douglas M. R., and Eckhard A. 1998. Efficiencies of transcritical CO_2 cycles with and without an expansion turbine. Int. J, Refrig. Vol. 21, No, 7, pp. 577-589.

Douglas. M. R. 2000. Modeling of carbon dioxide based air-to-air air conditioner. Ph.D. thesis, Purdue University.

Fagerli B.1997. On the feasibility of compressing CO_2 as working fluid in hermetic reciprocating compressor Dr Ing Thesis. Department of refrigeration and air conditioning, Norwegian University of Science and Technology, Norway.

Gnielinski, V., 1970. New equations for Heat and Mass Transfer in Turbulent Pipe and Channel Flow. International Chemical Engineer. 16, 359-368.

Gordon J, (technical editor), 2005. Cooling systems: Variable Displacement A/C Compressor. Electronic source, http://www.motorage.com.

Hashimoto, K. and Saikawa, M., 1997. Preliminary experimental results of CO_2 gas-cooling over-all heat transfer coefficient under supercritical condition. Presented at International Conference on Heat Transfer Issues in Natural Refrigerants, College Park, MD. 6-7 November.

Hwang Y. Doctor of philosophy. 1997. Comprehensive investigation of carbon dioxide refrigeration cycle. PhD thesis, University of Maryland.

Hwang Y.,and Radermacher R. 1998. Theoretical evaluation of carbon dioxide refrigeration cycle. HVAC&R. Vol. 4, No. 3. July.

Jordan C. R., and Priester G. B., 1969. Refrigeration and air conditioning. (Book). Prentice- Hall, NJ, 2nd Ed.

Kim M. H., Pettersen J., and Bullard C. W. 2004, Fundamental process and system design issues in CO_2 vapor compression system. Progress in Energy and Combustion Science 30, pp. 119-174.

Kim S. G., and Kim M. S. 2002. Experiment and simulation on the performance of an autocascade refrigeration system using carbon dioxide as refrigerant. Int. J. Refrig 25, 1093-1101.

Kline, S. J. and McClintock, F. A. 1953. Describing uncertainties in single-sampleexperiments. Mechanical Engineering, Vol. 75, pp.3-8.

Kuange G, Ohadi M. M., and Zhao V., 2004, Experimental study on gas cooling heat transfer for supercritical CO_2 in microchannels. Conference on Microchannels and Minichannels (ICMM 2004) June 17-19, Rochester, New York USA.

Liao S.M., Zhao T.S., and Jakobsen A. 2000. A correlation of optimal heat rejection pressures in transcritical carbon dioxide cycles. Applied Thermal Engineering. 20, pp.831-841.

Liu H., Chen J. P. and Chen Z. 2005. Experimental investigation of a CO_2 automotive air conditioner. Int. J. Refrig. 28, pp. 1293- 1310.

Lorentzan G. 1995. The use of natural refrigerants: a complete solution to the CFC/HCFC predicament. Int. J. Refrig Vol 18. No. 3, pp 190-197.

Lorentzen G., and Pettersen J.1992, A new efficient and environmentally benign system for car air conditioning. NTH-SINTEF Refrigeration Engineering, N-7034 Trondheim, Norway.

Lorentzen, G. and Pettersen, J., 1992. New possibilities for non CFC refrigeration. In proceedings of IRR international symposium on refrigeration, energy and environment. Trondheim. Norway, 22-24, June, pp. 147-163.

Molina M. J., and Roland F. S. 1974. Stratospheric sink for chlorofluoromethanes: chlorine atomic-atalysed destruction of ozone, Nature 249, p. 810-812.

Neksa P. 2004. CO_2 as refrigerant for systems in transcritical operation, principles and technology status. AIRH's Natural Refrigerant Conference, held at Museum of Sydney July 28.

Pettersen J., Hafner A., and Skaugen G. 1998. Development of compact heat exchangers for CO_2 air conditioning systems. Int. J. Refrig. Vol.21. No.3 pp180-193.

Pettersen. J. 1997. Experimental results of carbon dioxide in compression system. ASHRAE/ NIST conference. Refrigeration for the 21st century Gaithersburg, MD; pp. 27-37.

Preissner M., Cutler B., Singanamalla S., Hwang Y., and Radermacher R. 2000 Comparison of automotive air conditioning systems operating with CO_2 and R134a. Final proceeding of the 4th IIR-Gustav L. conference one natural working fluids at Purau (West Lafayette IN)25-28 July.

Rieberer, R. and Halozan, H., 1997. Design of heat exchangers for CO_2 heat pump water heater. Presented at International Conference on heat transfer issues in Natural Refrigerants College Park, MD, 6-7 November.

Solberg J. and Miller N. R. 1998. Digital Control of a Mobile Air Conditioning System. Electronic Source;

http://lims.mech.northwestern.edu/students/solberg/old_class_files/solberg313 control AC.pdf.

Steven J. B., Samuel F., Yana-Motta, and Piotra A. 2002. Comparative analysis of an automotive air conditioning systems operating with CO_2 and R-134a. Int. J. Refrig. 25, pp. 19-32.

Süß J. and Kruse H. 1998. Efficiency of the indicated process of CO_2 compressors. Int. J. Refrig. Vol.21, No.3, pp. 194-201.

Yin J. M., Bullard C. W., and Hrnjak. P. S., 2002. Design strategies for R744 gas coolers. Proceedings of the International Refrigeration Conference at Purdue, West Lafayette, IN.p 315-22.

APPENDIX A: UNCERTAINTY ANALYSIS AND ERROR ESTIMATION

An experimental work involves some physical variables. Measurements of these variables may involve measurement errors, which bring on uncertainty in the correctness of the values resulting from the measurement. The propagation of uncertainties is determined by using the method of Kline and McClintock (1953).

Errors basically grouped into two categories; bias and precision errors. The bias and precision errors are estimated by the following method:

$$B = \sqrt{\sum B_x^2} \quad x = 1,2,3,....N$$

(A.1)

$$P = \sqrt{\sum P_y^2} \quad y = 1,2,3,.....N$$

(A.2)

Where x and y are the total number of error sources in bias and precision errors respectively. The measurement uncertainty in x, Ux, is the combination of bias and precision uncertainty.

$$Ux = \sqrt{B^2 + P^2}$$

(A.3) where P is the estimate of precision uncertainty at 95% confidence/ limit.

The root sum square (RSS) method is used to determine the uncertainty U of the dependent parameters that were calculated from the measured independent variables. The relation between the dependent parameters and the independent variables can be estimated as:

$$N = f(N_1, N_2, N_3, ... N_N),$$

(A.4)

where $\frac{\partial N}{\partial N_i}$ i = 1,2,3, ..., is the derivative of the relation given in (A.4).

and the absolute uncertainty can be estimated as:

$$UN=\sqrt{\left(\frac{\partial N}{\partial N_1}UN_1\right)^2+\left(\frac{\partial N}{\partial N_2}UN_2\right)^2+\left(\frac{\partial N}{\partial N_3}UN_3\right)^2+....}$$

(A.5)

and the uncertainties of the independent parameters (U_{N1}, U_{N2}, U_{N3}, ...)

A.1 UNCERTAINTY IN MEASUREMENT OF REFRIGERANT TEMPERATURE

The refrigerant temperatures were measured using RTDs plug in type inserted into the tubing, the RTDs was in direct contact with the refrigerant. The RTDs are of class "A" platinum element. The RTD has an accuracy of ± 0.06% at 0°C and (DIN 43760 class A) and its linearity error can be estimated according to (Eq dT+ = ±0.15 + 0.002.|T|), DIN EN 60751 for class B and A,

$$B=\sqrt{(0.06T)^2+(0.15+0.002T)^2}$$

The RTDs are connected to a (DAQ) data acquisition system made by National Instrument, the NI card has a resolution of 0.000015°C, accuracy of 0.0052T°C and a precision error of 0.00219°C, the total bias error of the (DAQ) was estimated to be:

$$B=\sqrt{(0.0052T)^2+0.000015^2}$$

$P = 0.00219°C$

The overall uncertainty of the RTD can be calculated as

$$U=\sqrt{B^2+P^2}$$

A.2 UNCERTAINTY IN MEASUREMENT OF AIR TEMPERATURE

The air temperature at the inlet and outlet of evaporator are measured using thermocouples type T, voltage signals from thermocouples are collected by a data

acquisition system and translated into temperature readings. For the thermocouples an accuracy of 1°C and resolution of 0.025°C were considered.

$$B = \sqrt{1^2 + (0.025)^2} = 1.0003\,°C$$

Two thermocouples were fixed upstream of evaporator and four thermocouples were fixed downstream of evaporator, they are located at different points, a precision error of 0.05°C was considered due to this spatial variation.

$$U = \sqrt{B^2 + P^2}$$

$$U = \sqrt{1.0003^2 + 0.05^2} = 1.0015°C$$

A.3 UNCERTAINTY IN MEASUREMENT OF WATER TEMPERATURE

Thermocouples were inserted in the inlet, outlet pipes of the water tank and inside the water tank to measure water temperatures downstream and upstream the gas cooler, a bias error of 1°C and resolution of 0.025°C were considered. Various probes have different wire length and this may cause some error, to estimate for this error a value of 0.01°C is considered.

$$B = \sqrt{1^2 + 0.025^2 + 0.01^2} = 1.005°C$$

The thermocouples were placed at various locations inside the water tank; due to this spatial difference a precision error of 0.05°C is considered.

$$U = \sqrt{B^2 + P^2}$$

$$U = \sqrt{(1.005)^2 + (0.05)^2} = 1.005°C$$

A.4 UNCERTAINTY IN MEASUREMENT OF WATER MASS FLOW RATE

A.4.1 Uncertainty in Using Bucket and Weigh

The weigh used in the experiment has a resolution of 0.01 kg and an accuracy of 0.01 kg. the bias error can be estimated as:

$$B = \sqrt{0.01^2 + 0.005^2} = 0.011 \text{ kg}$$

a human error associated to the use of the bucket in handling water, a precision error of 0.01 kg is assumed.

$$U = \sqrt{0.011^2 + 0.01^2} = 0.0141 \text{ kg}$$

A.4.2 Uncertainty in Using Stopwatch

The stopwatch has an accuracy of 0.5 second, a resolution of 0.5 second and a digital error of 0.05 second which is one half times the least digit of the watch. A precision error of 1 second is considered for human error in using the stop watch.

$$B = \sqrt{0.5^2 + 0.25^2 + 0.05^2} = 0.561 \text{ sec}$$

$$U = \sqrt{0.561^2 + 1^2} = 1.1466 \text{ sec}$$

A.5 UNCERTAINTY IN MEASUREMENT OF REFRIGERANT PRESSURE

Pressure transducers were used to measure the refrigerant pressure on the low side and high side pressures, the low pressure transducer has a range of 0 to 6.8 MPa, and the high pressure transducer has a range of 0 to 20 MPa, both has an accuracy of 0.25% of reading. Display units are used to show pressure readings, both has an accuracy of 0.03% reading.

$$B = \sqrt{(0.0025P)^2 + (0.0003P^2)}$$

A precision error of 6917 Pa is introduced based on the response of the last digit of the display unit.

A.6 UNCERTAINTY IN MEASUREMENT OF REFRIGERANT MASS FLOW RATE

A coriolis mass flow meter is used to measure the refrigerant mass flow rate; the device has an accuracy of 0.03 kg/min and a resolution of 0.3 kg/min.

$$B = \sqrt{(0.03)^2 + (0.15)^2} = 0.153 \text{ kg/min}$$

The mass flow rate readings were fluctuating, this error is considered to be precision error and a value of 0.01kg/min is considered.

$$U = \sqrt{(0.153)^2 + (0.01)^2} = 0.1533 \text{ kg/min}$$

VITA AUCTORIS

Mowafaq Abdallah was born in 1956 in Baghdad, Iraq. He graduated from Almarkaziyah High School in 1974. From there he went on to the University of Baghdad where he obtained a B.Sc. in Mechanical Engineering in 1978. From 1980 to 2003 he served as a Mechanical Engineer in professional field. He is currently a candidate for the Master's degree in Mechanical Engineering at the University of Windsor and hopes to graduate in Fall 2006.